Tests to Failure with Increasing Loads of the AASHO Test Bridges

CHARLES F. GALAMBOS and GEORGE S. VINCENT
Respectively, Bridge Engineer, and Chief, Bridge Research Branch, Bureau of Public Roads

This paper describes the tests to failure of the ten test bridges remaining in operation at the end of regular testing on the AASHO Road Test. The bridges failed under increasingly heavier moving loads. A brief description of the test vehicles, testing procedure and instrumentation is presented. The behavior during the test and under failure of a noncomposite steel bridge, composite steel bridge, reinforced concrete bridge, post-tensioned prestressed concrete bridge and a pretensioned prestressed concrete bridge is described in detail. Computed ultimate moments are compared with the moments produced by the test vehicles and the dead weight of the bridges.

• It is assumed that the reader is at least partially familiar with the AASHO Road Test. Further details can be found in "AASHO Road Test Report 4" (HRB Special Report 61D, 1962).

Of the 18 test bridges constructed on the AASHO Road Test, 13 remained in operation at the end of the regular test traffic in November 1960. Three of these bridges were destroyed by the accelerated fatigue tests conducted in the winter of 1960-61. This left 10 bridges, which included 3 noncomposite steel bridges (1A, 9A, 9B), 1 composite steel bridge (3B), 2 reinforced concrete bridges (8A and 8B) and 4 prestressed concrete bridges (5A, 5B, 6A and 6B). Two of the latter (6A, 6B) contained pretensioned strands and the others (5A, 5B) contained post-tensioned cables.

The tests to failure were conducted at intervals, beginning in March 1961 and ending in June 1961. Five test vehicles were employed, a tandem axle truck (No. 62) used during regular testing, a Caterpillar tractor-scraper earth mover (No. 96) and three tank carriers (Nos. 97, 98 and 99). The vehicles are shown in Figure 1. The truck and carriers (Nos. 98 and 99) were used only to a limited extent. Most of the testing to failure was done with tank carrier No. 97. This vehicle was made available to the Road Test by the U.S. Army Transportation Corps specifically for these tests.

This report describes the tests in general and, in more detail, the behavior during testing and failure of each type of bridge, to make comparisons between bridges where applicable and to compare the theoretical ultimate moments with those calculated from the measured axle loads of the test vehicle.

Failure for the various types of bridges is defined as follows:

All steel bridges (both composite and noncomposite) were considered to have failed whenever the permanent deformation, as measured at midspan, increased at an increasing rate at each successive passage of the test vehicle.

The reinforced concrete bridges and one of the post-tensioned prestressed concrete bridges (5A) failed when there was visible crushing of the deck concrete near midspan.

The other prestressed concrete bridges failed when the tensile reinforcement ruptured near midspan.

The test bridges were placed in groups of four, each bridge providing one traffic lane. The four bridges at each location were supported on a common concrete substructure consisting of two abutments and one pier. The piers and abutments for all bridges were identical in all major details. They were supported on spread footings located on a hard-clay till.

Each bridge superstructure consisted of three identical beams, an exterior beam near the outside edge of the roadway, a center beam, and an interior beam near the center of the roadway. The three beams were simply supported on a 50-ft span and carried a reinforced concrete slab 6½ in. thick and 15 ft wide. The slab was separated from the adjacent bridges and the backwall of the abutment by 1-in. clear space and was provided with a 12- by 12-in. timber curb bolted to the outside edge. Figure 2 shows a typical test bridge location.

TEST VEHICLE, TESTING PROCEDURE AND INSTRUMENTATION

Test Vehicle

The over-all dimensions and axle spacings of tank carrier No. 97 are shown in Figure 3 along with the empty axle weights and the maximum gross axle weights. Figure 4 shows several views of this test vehicle.

Whenever reference is made to "axle loads" or "axle weights", the vehicle was considered to have 7 axles. Actually, the configuration of the last three axles was quite complicated and consisted of three pairs of trunion axles with equalizer bars arranged so as to result in equal axle loading within a vertical movement of 7 in., up or down, from normal level position. In other words, the last 3 axles were really 6 "half axles" each supported by 4 wheels.

In calculating moments based on axle weights, it was assumed that the axle loads were transferred to the bridge as line loads. Actually, especially for the last three axles, the load was probably more a distributed load than three line loads. This was due to the close axle spacings (4.3 ft), the many tires (a total of 24) and the width of the test vehicle. The distance out-to-out of tires was nearly 12 ft and the traveled way on all test bridges was 14 ft.

The concrete blocks used for loading the regular test vehicles were also utilized for loading the tank carrier. These blocks weighed about 2,500 lb each and were placed on the rear platform of the test vehicle. In order to cause failure in the strongest bridges, a more dense material than concrete had to be used as a load. A combination of steel ingots and concrete blocks proved to provide sufficient load.

The heaviest load placed on the vehicle resulted in gross axle loads of 72.3 kips, 73.5 kips and 82.3 kips, respectively, for the last three axles.

All of the test bridges were 50 ft long and, therefore, the whole test vehicle could barely be placed on a bridge at one time. For the purpose of computing the midspan static moments, only the last three axles were used. Whenever the third point and end-of-cover plate moments were desired, the effect of the third and fourth axles was also included in the computations.

Testing Procedure

The tests to failure with increasing loads followed the same pattern as was used during regular test traffic. That is, the direction, speed and lateral position of the test vehicle were the same. The vehicle speed was approximately 30 mph, except on the heavier loadings where the speed was reduced.

A "loading" in this report is defined as one particular set of axle loads. The terms "trip" and "run" are used interchangeably and are defined as a single passage of the test vehicle over the test structure.

The testing sequence was a follows: With

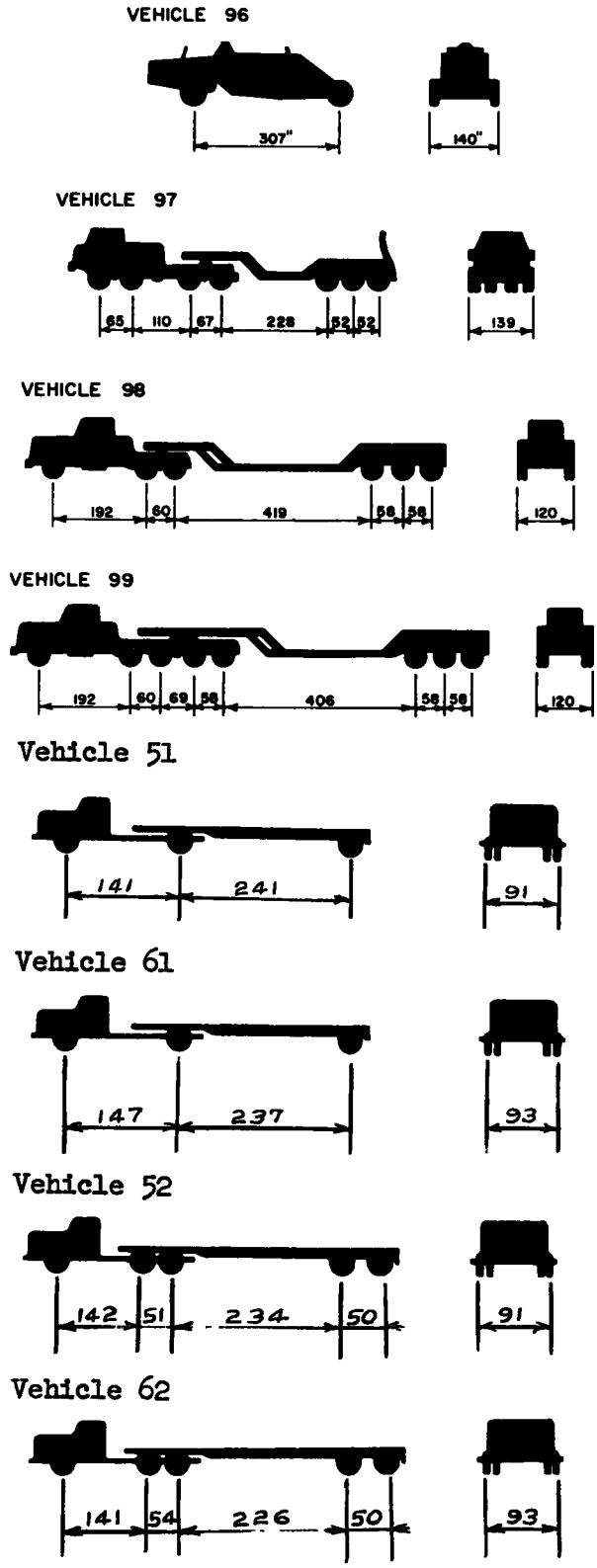

Figure 1. Diagrams of test vehicles.

Figure 2. Typical test bridge location.

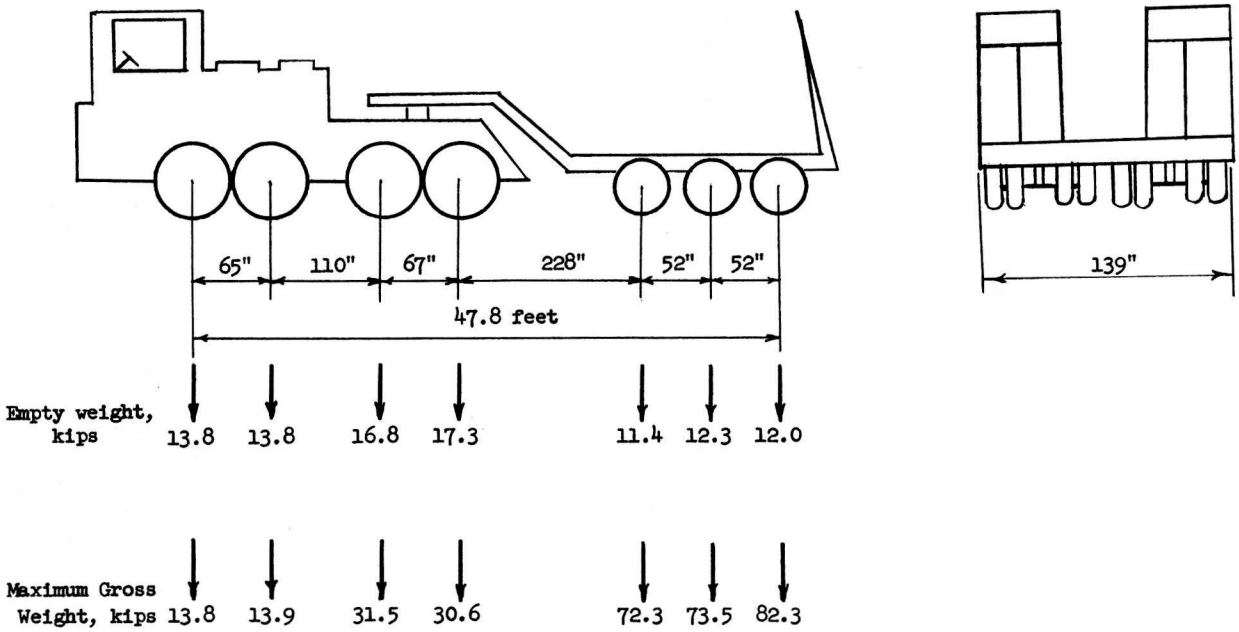

Figure 3. Test vehicle weights and dimensions.

the first loading (which produced about the same midspan moment as the regular test vehicle) 30 runs were made. Strain and deflection measurements were made and the behavior of the bridge was observed. Next, the test vehicle was loaded to a higher loading, 30 runs were made and the same measurements were repeated. This sequence of loading, 30 runs, higher loading, 30 runs, etc., was repeated until the bridge failed.

The number of runs was arbitrarily chosen with the thought in mind that 30 runs during one loading were enough to establish a pattern of behavior of the bridge. Usually, 3 or 4 of

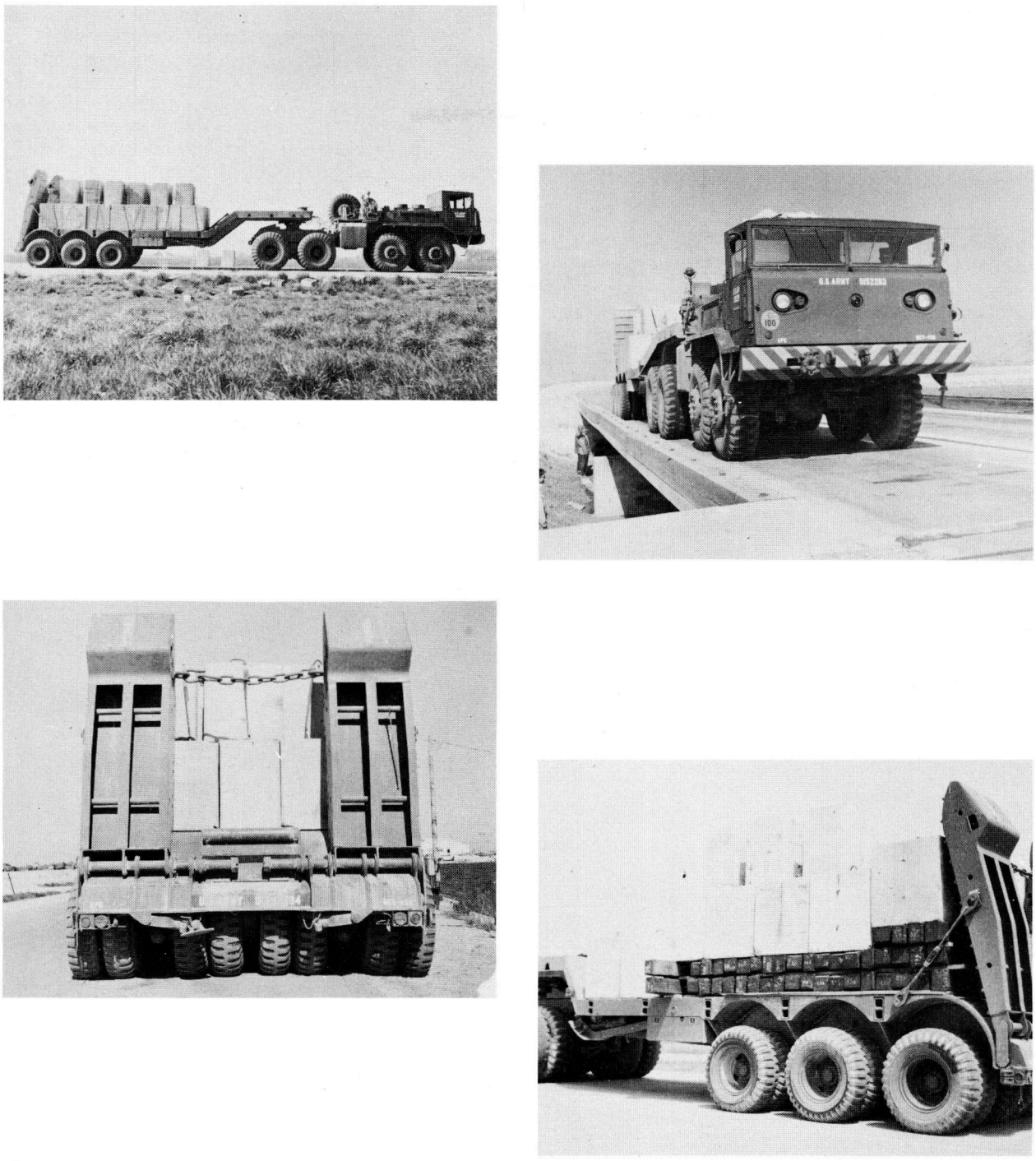

Figure 4. Test vehicle No. 97.

the 30 runs were made at creep speed so that the magnitude of impact could be determined.

The number of loadings varied from 3 loadings for one bridge to as high as 14 loadings for another bridge. To minimize handling of the load, the same loading was used on several bridges. Therefore, what constituted a substantial increase of load for one bridge was a relatively small increase in load for a stronger bridge. However, enough loadings were always used to determine the moment-deflection and moment-strain relationship.

Instrumentation

The bridge beams were instrumented for measurement of strains and deflections caused by vehicles. The transducers for determination of transient strains were electric-resistance strain gages bonded to the beams at midspan and several other locations. The detailed gage locations are described in Section 2.3 of the AASHO Road Test Report 4 (HRB Special Report 61D).

The gages were bonded to the surface of steel beams, to the prestressing steel or the surface of the concrete on prestressed concrete beams, and to the reinforcing bars in the reinforced concrete beams. The gages were placed on or near bottom of the beams at all locations, except that there were two additional gages at midspan located at or near the underside of the slab.

The transient deflections were measured with demountable cantilever beams equipped with bonded electric resistance strain gages, but as these devices were designed to measure deflections produced by the regular test traffic, their range was quickly exceeded during the tests to failure with increasing loads. Another device, a slip ring deflectometer, was therefore used for measuring maximum deflections.

The strain gages bonded to the beams formed one or two arms of an external Wheatstone bridge; the remaining arms were provided by appropriate dummy gages, and the Wheatstone bridge was connected through amplifiers to recording oscillographs. In like manner, the four gages on the cantilever deflectometers also made up an external Wheatstone bridge which was connected to the oscillographs.

As long as the bonded gages and the cantilever deflectometers were operative, the midspan lower flange strains and deflections and the strains just off the ends of the cover plates were measured on about every fifth run. However, the main source of test data was the slip ring deflectometer. This simple device consisted of a fork attached to the underside of a beam, a rod supported on the ground and extending through the prongs of the fork and a ring sliding along the rod.

A slip ring deflectometer was placed under each of the three beams of each bridge and by measuring with a ruler to the nearest 0.02 in., the position of the ring relative to a fixed datum before and after each run, (a) the live load deflection, (b) the permanent deformation due to the preceding run, and (c) the cumulative permanent deformation could be deter-

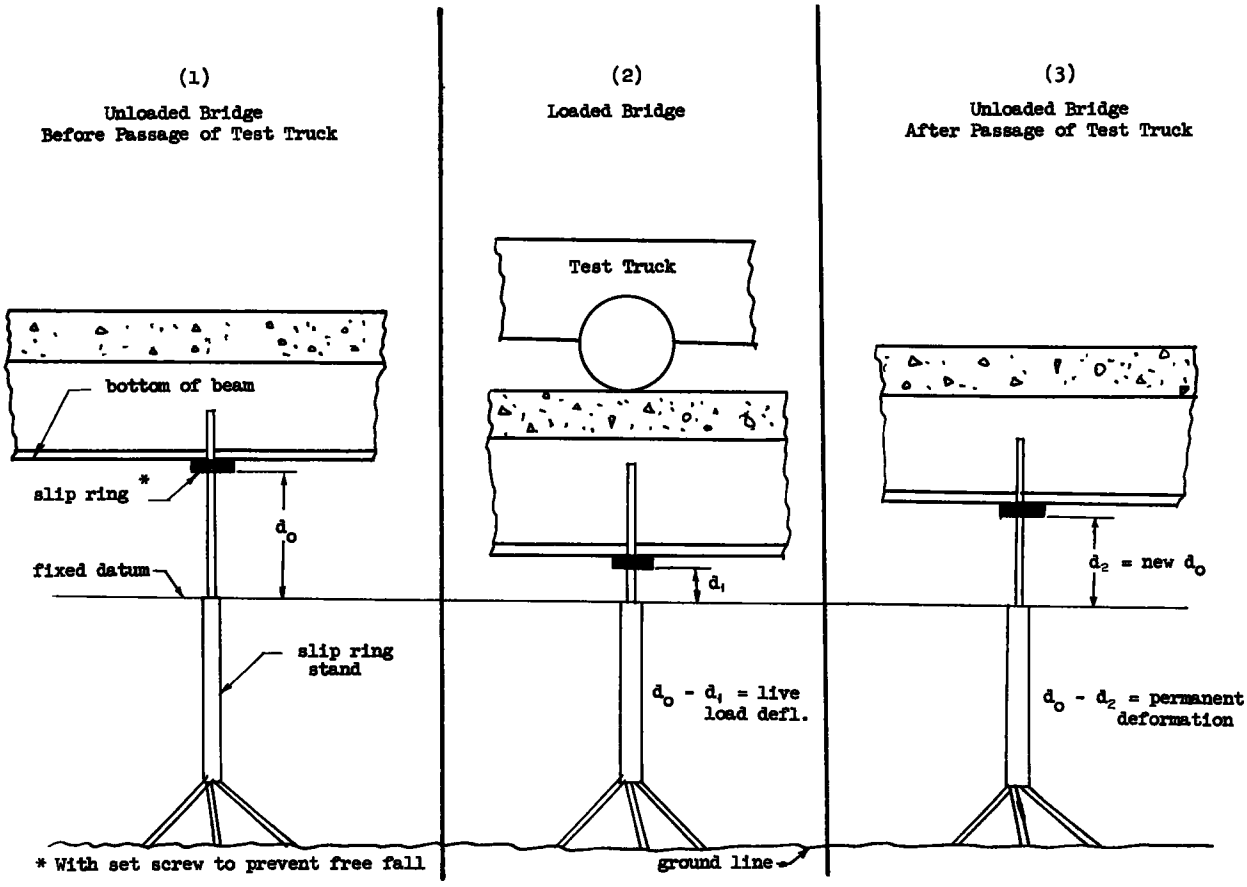

Figure 5. Slip-ring deflectometer.

mined. The ring was pushed by hand snugly up against the bottom of the fork after each run. To prevent the ring from falling freely, it was provided with a set screw which could be adjusted to produce the desirable close fit. Figure 5 shows the sequence of measurements made with this device.

BEHAVIOR UNDER TESTING AND FAILURE OF BRIDGES

Noncomposite Steel Bridge 9A

The behavior under testing and failure of bridge 9A was quite typical of the other two noncomposite bridges.

A typical cross-section at midspan and other details of a noncomposite bridge are shown in Figure 6. All cover plates were 6 in. by $\frac{7}{16}$ in. and were placed on the top and bottom of the beams on bridges 9A and 9B and only on the bottom of bridge 1A.

The yield points as determined from laboratory tests on coupons taken from the flanges and the web of the beams for bridge 9A were 32.5 ksi for the flanges and 36.1 ksi for the web. The coupons were tested in tension to failure at a speed of 0.104 in. per min. up to yielding. All rolled beams and cover plates were made of structural carbon steel meeting the requirements of ASTM Designation A7-55T.

During the time of regular test traffic bridge 9A was subjected to 477,900 passages of the most heavily loaded tandem axle vehicles (a diagram of such a typical vehicle, No. 62, is shown in Fig. 1). The nominal axle weights of this vehicle during regular testing were 12 kips on the front axle and 48 kips on each set of tandem axles. The gross weight of the vehicle was therefore about 108 kips.

The maximum mean live load stress in the bottom fibers near the end of the cover plates caused by regular test traffic was about 14.6 ksi. This value was obtained by averaging the mean stresses of all three beams at both ends of the cover plates. The corresponding calculated dead load stress, based on measured weights and dimensions of the various bridge components was about 10.3 ksi. The total stress, recorded live load plus calculated dead load, was approximately 24.9 ksi.

The general condition of the bridge at the start of the tests to failure with increasing loads was as follows. The slab was badly cracked, especially near the ends of the cover plates. There were two tiny fatigue cracks at the toes of the welds on both sides of the cover plate at the exit end on the exterior beam. It is believed that none of the above mentioned conditions had any marked effect on the behavior of the bridge during the test to failure.

Five loadings were used. The axle loads, varying from 23 kips to 45 kips on each rear axle, as well as the maximum static midspan and end of cover plate moments, computed from the axle loads, are given in Table 1. For the purpose of comparison, the axle loads and calculated moments produced by regular test vehicle No. 62, along with the computed dead load moments are included. All values are static values, no impact is included.

The increments of loading were quite uniform, in that each loading increased the moments by approximately 200 ft-kips.

Table 2 gives the recorded live load stresses and deflections for each loading and the computed dead load stresses and the stresses and deflections produced by regular test vehicle No. 62. The deflections are elastic live load deflections at midspan obtained from slip ring measurements. The values shown are averages for all three beams; only those runs which were made at approximately the same speed entered into the computations.

The stresses shown are extreme fiber stresses obtained from strain measurements. The values are averages for all three beams and again only those runs which were made at the same speed were used in the computations. The numbers in parentheses, when added to the corresponding dead load stress, exceed the yield point of the material. They are not true stresses and serve only to indicate the rate of yielding.

TABLE 1

COMPUTED MAXIMUM STATIC MOMENTS AND MEASURED AXLE LOADS, BRIDGE 9A

Load	No. of Runs	Midspan Moment (ft-kips)	End of Cover Plate Moment (ft-kips)	Axle Loads (kips)						
				1	2	3	4	5	6	7
Dead		521	461							
Veh 62[1]		590	620	10 9	24 4	24 4	24 1	24 2		
1	30	760	740	14 1	14 2	16 9	17 0	21 8	23 2	23 0
2	30	1,010	960	14 8	14 4	17 4	17 1	28 0	30 1	33 4
3	30	1,230	1,160	14 1	13 8	19 6	20 7	35 8	36 6	38 9
4	30	1,390	1,320	14 1	14 3	23 2	24 2	41 6	41 1	43 3
5	20	1,535	1,490	13 8	13 8	28 8	29 0	42 8	45 4	50 2

[1] Regular test vehicle 62.

TABLE 2

STRESSES AND DEFLECTIONS, BRIDGE 9A

Load	Elastic Live Load Deflection (in.)	Stresses[1] (ksi)								
		Midspan Lower			Exit End Cover Plate			Entrance End Cover Plate		
		Int. Beam	Center Beam	Ext. Beam	Int. Beam	Center Beam	Ext Beam	Int. Beam	Center Beam	Ext. Beam
Dead, stress		7 9	9 5	11 1	8 5	10 3	12 0	8 5	10 3	12 0
Veh 62[2]	2 0	—	—	—	15 4	14 6	13 6	15 5	14 8	13 5
1	2 0	13 7	14 0	13 7	14 0	13 6	12 7	16 2	16 0	15 3
2	2 4	18 1	18 3	18 4	17 8	17 5	16 8	21 3	21 0	20 2
3	3 3	23 9	(24 0)	(24 7)	21 9	22 2	(24 8)	(26 6)	(27 3)	(25 3)
4	3 6	23 1	(24 5)	(25 7)	(24 3)	(24 5)	(25 6)	(26 9)	—	—
5[3]	4 5	(26 7)	(26 5)	(24 5)	(29 4)	(27 4)	(25 2)	—	—	—

[1] Yield point determined from coupon tests was 32.5 ksi; values in parentheses when added to the dead load stress exceed the yield point.
[2] Regular test vehicle 62.
[3] Slower speed, 20 mph.

In Figure 7a, the moment-deflection diagram, the calculated maximum static moment caused at midspan by the test vehicle is plotted as a function of the midspan cumulative deflection. The cumulative deflection is made up of elastic live load deflection and permanent set. Only the permanent deformations resulting from the test to failure are included. (Permanent set was observed on all the bridges during the two years of test traffic, but it is not included in Fig. 7.)

Usually 30 runs were made with each loading. If the number of runs differed from 30, it is so indicated. The average live load deflection (a mean value of all three beams) during those loadings that did not produce a permanent deformation is represented by a dot for each such loading. The dots are connected with each other and the origin by a straight line. The parallelogram shaped areas resulted from the loadings that produced permanent set in the bridge. For each such area, the upper left corner represents the deflection (both live load and permanent set) due to the first run of a particular loading and the upper right corner is the deflection produced by the last run of the same loading. The lower right corner represents the accumulated permanent set for this and all previous loadings.

An additional scale is shown at the right of each moment-deflection diagram. The scale expresses the total external moment, M (including maximum static moment and dead load moment), at midspan in terms of the moment corresponding to the design stress currently allowed by bridge specifications. The magnitude of this allowable stress is indicated by the subscript; for example, M_{18} represents moment corresponding to a design stress of 18 ksi.

Figure 7b, the set-trip diagram, plots the permanent set at midspan as a function of the number of trips of the test vehicle; both are plotted cumulatively. The load number and the nominal vehicle speed are shown at the top.

With reference to Figure 7 and to the table of stresses and axle loads, the description of the behavior of the bridge during testing follows.

The first two loadings produced no permanent deformation and no yielding was noted anywhere. However, yield lines were noted on the bottom flanges on all three beams near the entrance end of the cover plates during the third loading. The presence of yielding could be observed by the flaking off of the paint along straight lines, which is characteristic of yielding of steel. The first run, at creep speed, produced a permanent set at midspan in all three beams of 0.06 in. The rate of permanent deformation (the trip by trip set) for the subsequent 30-mph runs was quite uniform, being about 0.02 in. per run, and the total permanent deformation for 30 runs was about 0.75 in.

The uniformity of the recorded strains and of the rate of permanent deformation during the speed runs following the first creep run indicates that the material was undergoing strain hardening.

The third loading, in which yielding was first observed, produced a calculated total (live plus dead load) static midspan moment of 1,751 ft-kips and a corresponding moment at the end of the cover plates of 1,621 ft-kips. These values were respectively 58 percent and 50 percent above the moments produced by regular test vehicle No. 62. They are static values and contain no effects due to impact.

Inspection of the bridge after the runs of the fourth loading showed yielding near both ends of the cover plates in the lower flanges and also at the same points in the upper flanges. As yet no yielding was discovered near midspan.

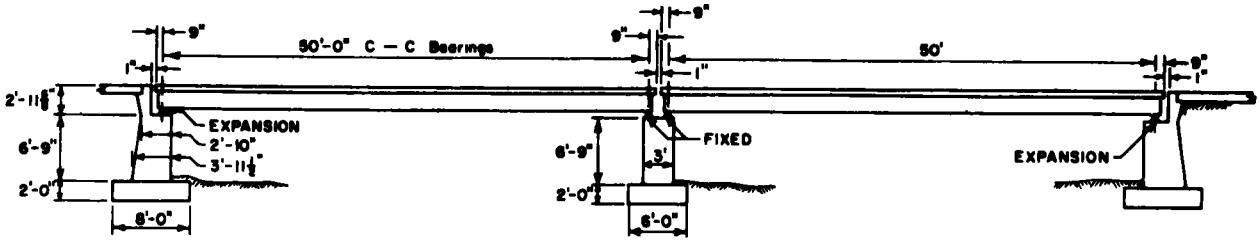

Typical Longitudinal Section

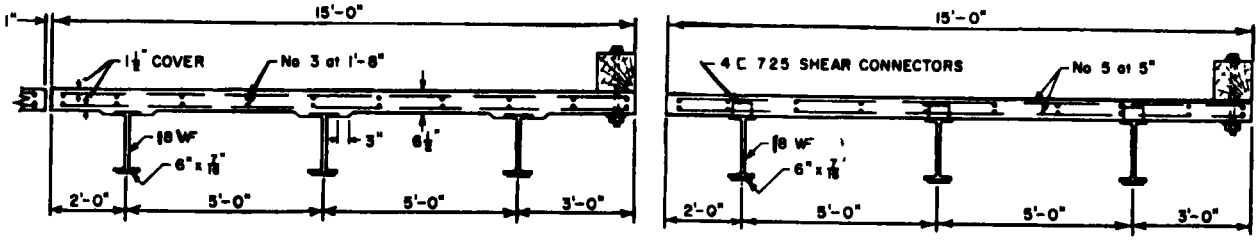

Noncomposite Section at Midspan
Bridge 9A

Composite Section at Midspan
Bridge 3B

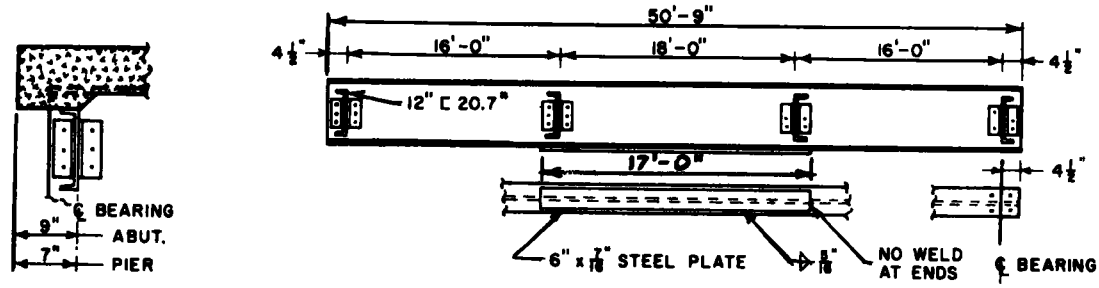

END OF SLAB

STEEL BEAM FOR NONCOMPOSITE BRIDGE 9A

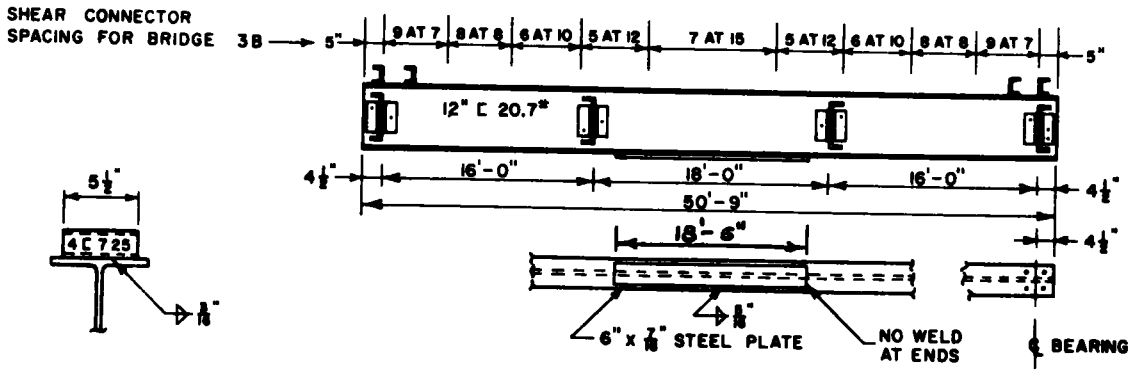

SHEAR CONNECTOR

STEEL BEAM FOR COMPOSITE BRIDGE 3B

Figure 6. Typical steel bridge sections and details.

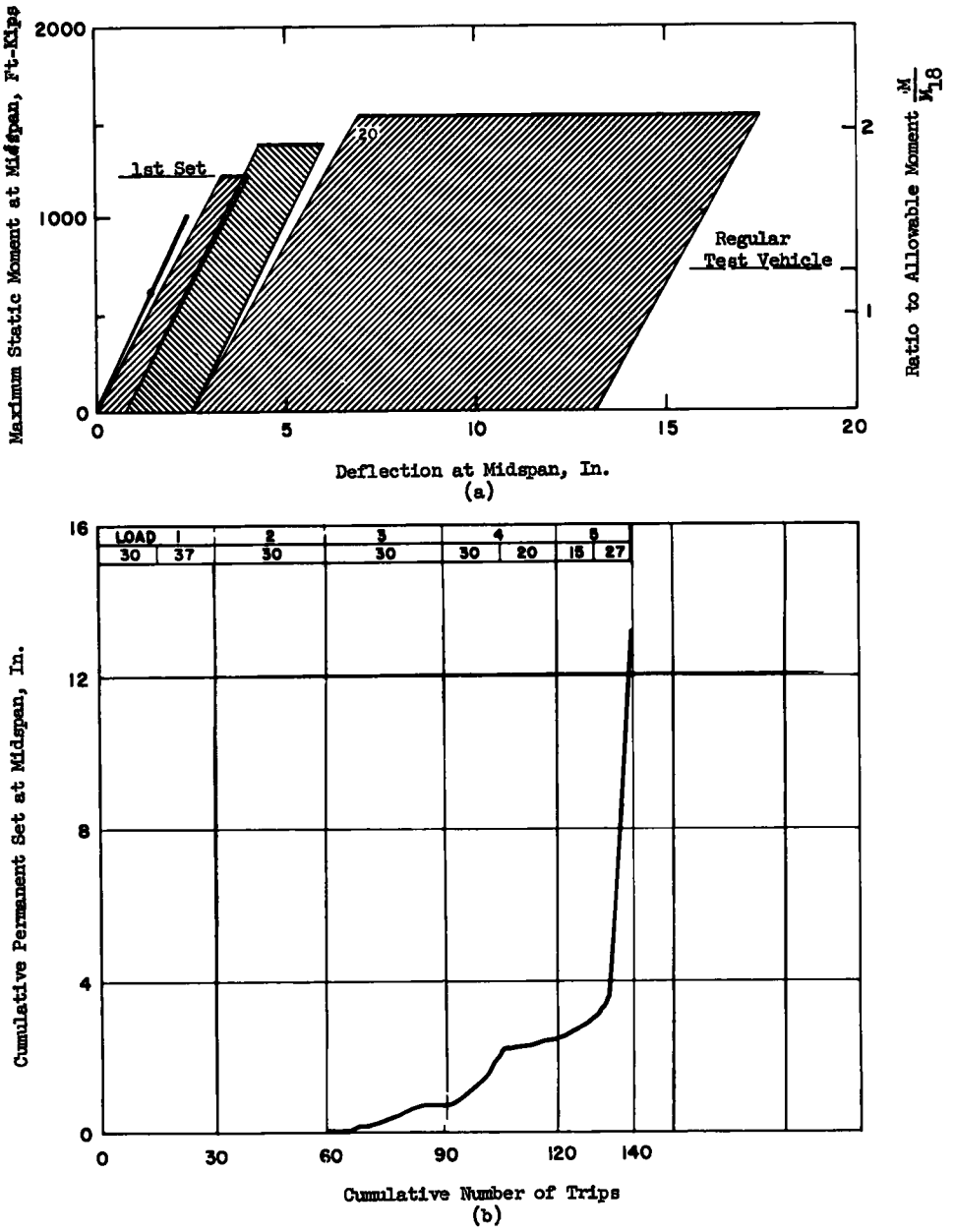

Figure 7. Moment-deflection and set-trip diagram, noncomposite steel bridge 9A.

The rate of permanent deformation during the fourth loading was about 0.13 in. per run for the first fifteen runs, but only 0.2 in. per run during the last 15 runs. The decrease coincides with the reduction of vehicle speed from 30 mph to 20 mph. The reduction in the permanent deformation is clearly evident in Figure 7b where a marked change in the slope of the curve is seen at the point denoting the change in vehicle speed.

Yielding of the cover plates near midspan was noted on all three beams after the third run of the fifth loading. The vehicle speed for the first 10 runs was held down to about 15 mph; the resulting permanent deformation per run was about 0.04 in. When the speed was increased to 27 mph, heavy yielding resulted and the permanent deformation became so large that the testing was stopped on the twentieth run. As much as 2 in. of permanent deformation per run was recorded on the last three runs and the total permanent deformation for all five loadings was approximately 13 in.

The test truck could have crossed the bridge several more times probably with even a heavier loading, but it was feared that the large dip in the deck and the sudden rise at the pier would harm the test vehicle. The condition of

the slab at the end of the test was judged to be about the same as described at the beginning of the test.

Figure 8 shows the bridge after failure and a typical plastic hinge near the ends of the cover plates. These plastic hinges developed first near the end of the cover plates at the entrance of the bridge, later at the end of the cover plates at the exit, and finally at midspan. By the time a plastic hinge was developed at midspan, the permanent deformation was increasing so rapidly that the bridge was declared failed (as defined earlier) and testing was stopped.

Inspection of the bridge at the end of the test showed that there were fine cracks on all three beams near both ends of the cover plates at the toes of all welds. It is believed that these were fatigue cracks, caused by regular test traffic, that became visible due to the extreme curvature of the beams.

The failure loading produced total calculated static midspan moments of 2,056 ft-kips and corresponding moment at the end of the cover plates of 1,951 ft-kips. These moments were respectively 85 percent and 80 percent above the moments produced by regular test vehicle No. 62. The weights of the last three axles during the failure loading were, 42.8, 45.4 and 50.2 kips—front to back, respectively.

Two other noncomposite steel bridges were tested to failure with increasing loads. One of them, bridge 9B, was similar in design and construction to bridge 9A and was adjacent to it. The same number of trips with the same loadings were made across both bridges up to the failure of bridge 9A. The loading under which yielding was first observed on 9B was also the third loading, producing total static moments at midspan that were 58 percent above those produced by the regular test vehicles. The corresponding yield moment at the end of the cover plates was 50 percent in excess. These percentages were the same as on bridge 9A. Bridge 9B failed under a slightly higher loading than bridge 9A. The rear axle weights of the test vehicle under the failure load were, front to back, 44.8, 46.5 and 51.2 kips. The total moment at failure at midspan and at the end of the cover plates was, respectively, 90 percent and 84 percent above that produced by the regular test vehicles. The total permanent set at midspan on bridge 9B was 12.5 in. and the total number of trips with all six loadings was 190, as compared with only 140 trips and five loadings on bridge 9A.

The third noncomposite bridge, 1A, was tested with 14 increasingly heavier loadings and three test vehicles. The yield load produced total midspan and end of cover plate moments that were 28 percent and 38 percent in excess of the corresponding moments produced by the regular test vehicle for this bridge, vehicle No. 51. The failing load produced corresponding moments 80 percent in excess at midspan and 73 percent in excess at the end of the cover plates. With the 14 loadings a total of 403 trips was made across the bridge and the total permanent set at midspan was about 18 in.

All three of the noncomposite bridges behaved similarly during the tests to failure with increasing loads.

Composite Steel Bridge 3B

The compositely built steel bridge was subjected to passages from the single-axle vehicles during the regular tests (vehicle No. 61, Fig. 1). The nominal axle loads were 9 kips on the front axle and 30 kips each on the other axles.

Typical sections of the composite bridge are shown in Figure 6. The cover plates were placed only on the bottom flanges of the beams and extended 1 ft beyond the theoretical ends. The flange yield point determined in the laboratory was 35.1 ksi, and the corresponding yield point for the web was 39.9 ksi. The mean dead load stress at the ends of the cover plates, calculated from measured beam and slab dimensions, was 15.9 ksi.

During the 26 months of testing with regular test traffic, this bridge was subjected to 557,800 passages of the regular test vehicles. Just before the test to failure the bridge was also subjected to various tests by special military vehicles.

Before testing to failure, the concrete deck, the abutment and the rockers were in very good condition. Some fatigue cracks were noted, one on the exterior beam near the exit end of the cover plate, about as long as the width of the weld (½ in.), and one larger crack on the interior beam near the entrance end of the cover plate on the interior side. This crack had broken through the flange and extended 1.6 in. from the edge of the flange toward the web. In other words, over 20 percent of the bottom flange was broken.

Nine loadings were made with three test vehicles, all of them being tank carriers. For loadings 1 through 4 tank transporters 98 and 99 were used and for loadings 5 through 9 the usual test vehicle (97) was employed.

The computed maximum static midspan and end of cover plate moments produced by these vehicles and the respective axle loads are given in Table 3. For comparison, the moments resulting from a regular test vehicle are also included.

The direction of travel of the test vehicles was the same as in the regular test traffic except as subsequently noted.

Figure 9 shows the moment-deflection relationship and the set-trip relationship. The general nature and interpretation of this figure is the same as has been described for the non-

TABLE 3

COMPUTED MAXIMUM STATIC MOMENTS AND MEASURED AXLE LOADS, BRIDGE 3B

Load	No. of Runs	Midspan Moment (ft-kips)	End of Cover Plate Moment (ft-kips)	Axle Loads (kips)							
				1	2	3	4	5	6	7	8
Dead		476	409								
Veh 61[1]		450	460	8 9	30 2	29 9					
1[2]	30	950	800	19 9	33 4	33 9	—	—	28 6	28 4	27 8
2[2]	9	1,080	930	17 2	21 9	22 5	28 0	28 3	33 3	32 8	32 6
3[2]	30	1,060	920	17 0	21 9	21 9	27 5	27 9	32 9	32 3	32 3
4[2]	30	1,050	910	20 8	42 5	43 3	—	—	32 2	31 6	31 8
5[3]	30	1,350	1,300	13 7	13 7	26 3	25 2	37 8	39 7	44 7	
6[3]	30	1,520	1,460	13 7	13 9	27 4	29 5	42 7	44 2	50 7	
7[3]	30	2,010	1,870	—	—	—	—	55 7	57 3	68 0	
8[3]	30	2,270	2,110	14 2	14 2	31 0	31 0	62 9	66 6	75 0	
9[3]	14	2,520	2,330	13 8	13 9	31 5	30 6	72 3	73 5	82 3	

[1] Regular test vehicle 61.
[2] Loadings 1–4, vehicle 98 and 99.
[3] Loadings 5–9, vehicle 97.

TABLE 4

STRESSES AND DEFLECTIONS, BRIDGE 3B

Load	Elastic Live Load Deflection (in.)	Stresses[1] (ksi)								
		Midspan Lower			Entrance End Cover Plate			Exit End Cover Plate		
		Ext. Beam	Center Beam	Int. Beam	Ext. Beam	Center Beam	Int. Beam	Ext. Beam	Center Beam	Int. Beam
Dead,		16 5	14 0	11 4	18 9	16 0	13 1	18 9	16 0	13 1
Veh 61[2]	0 84	—	—	—	12 3	13 0	12 8	12 4	12 5	12 6
1	1 18	17 6	16 9	17 5	(18 6)	16 8	16 2	(19 0)	17 3	16 1
2	1 13	(19 2)	16 9	15 2	(19 7)	16 5	15 9	(17 0)	16 5	16 4
3	1 40	(19 4)	20 0	21 8	(23 1)	(19 8)	20 5	(19 2)	—	19 7
4	1 45	(20 2)	20 8	22 7	(20 6)	(20 3)	21 3	(19 9)	(19 9)	19 9
5	1 68	(25 6)	(25 6)	(25 2)	(30 4)	(28 6)	(27 7)	(26 6)	—	(23 1)
6	2 11	(29 8)	(31 9)	(33 1)	(36 3)	(34 8)	(38 2)	(27 0)	—	(27 3)
7[3]	2 25	(35 0)	(33 3)	(30 5)	(47 8)	(46 3)	(39 8)	(49 4)	(44 9)	(39 9)
8	2 60				Gages out					
9	3.20				Gages out					

[1] Values in parentheses when added to the dead load stress exceed the yield point; flange yield point determined from coupon tests was 35 1 ksi.
[2] Regular test vehicle 61.
[3] Slower speed, 16 mph.

composite bridge. Table 4 gives the live load and dead load stresses and deflections. Again, the effects produced by regular test vehicle 61 are included to serve as a comparison.

The first loading produced no visible yielding. However, when the dead load stress is added to the recorded live load stress near both ends of the cover plate of the exterior beam, the resulting sum exceeds the yield point by over 2 ksi. There was also a trace of permanent set measured at midspan, amounting to about 0.09 in.

The next three loadings did not differ very much from each other and should be regarded as one loading. A total of 69 runs was made, and some yielding took place because the permanent deformation at midspan due to loadings 2, 3, and 4 was about 0.4 in. As yet no yield lines were visible anywhere with the unaided eye.

During the fifth loading yield lines began to appear on the bottom flange, first near the entrance end of the cover plates and later (25th trip) also near the exit end of the cover plates. The set-trip diagram, Figure 9b, shows that the rate of permanent deformation decreased after the twelfth run. There was no change in vehicle speed or direction, so the change in the rate of permanent deformation was inherent in the bridge.

The fatigue crack on the interior beam became noticeably wider during this loading but did not progress farther towards the web. The measured width of the crack at the edge of the flange was 0.07 in. after the fifth loading.

Yield lines appeared all along the lower flanges and on the bottom of the cover plates for their entire length during the sixth loading. The extremities of the bottom flange yielding were 8 ft from the ends of the bridge. Yielding

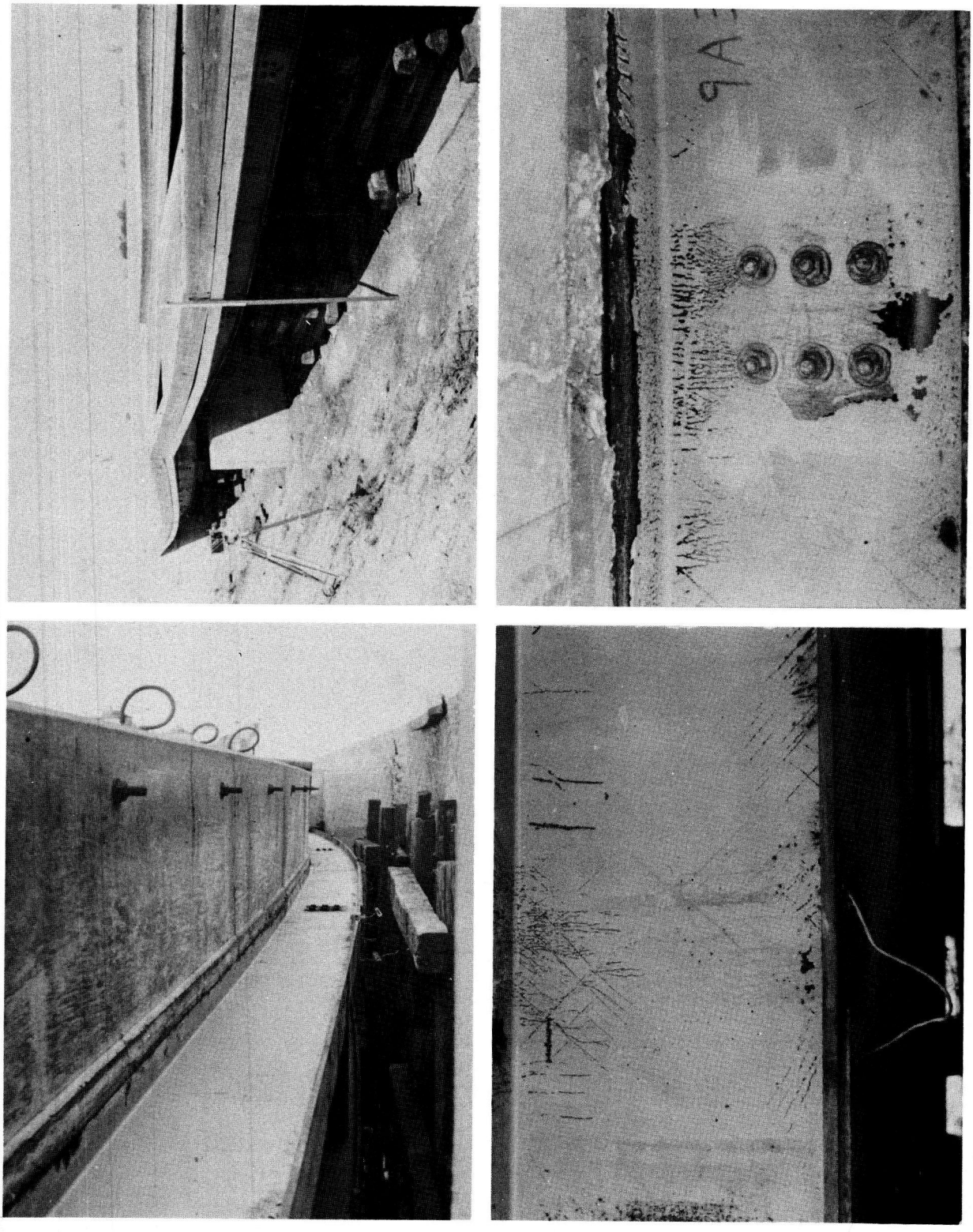

Figure 8. Noncomposite bridges after failure, yielding near end of plates.

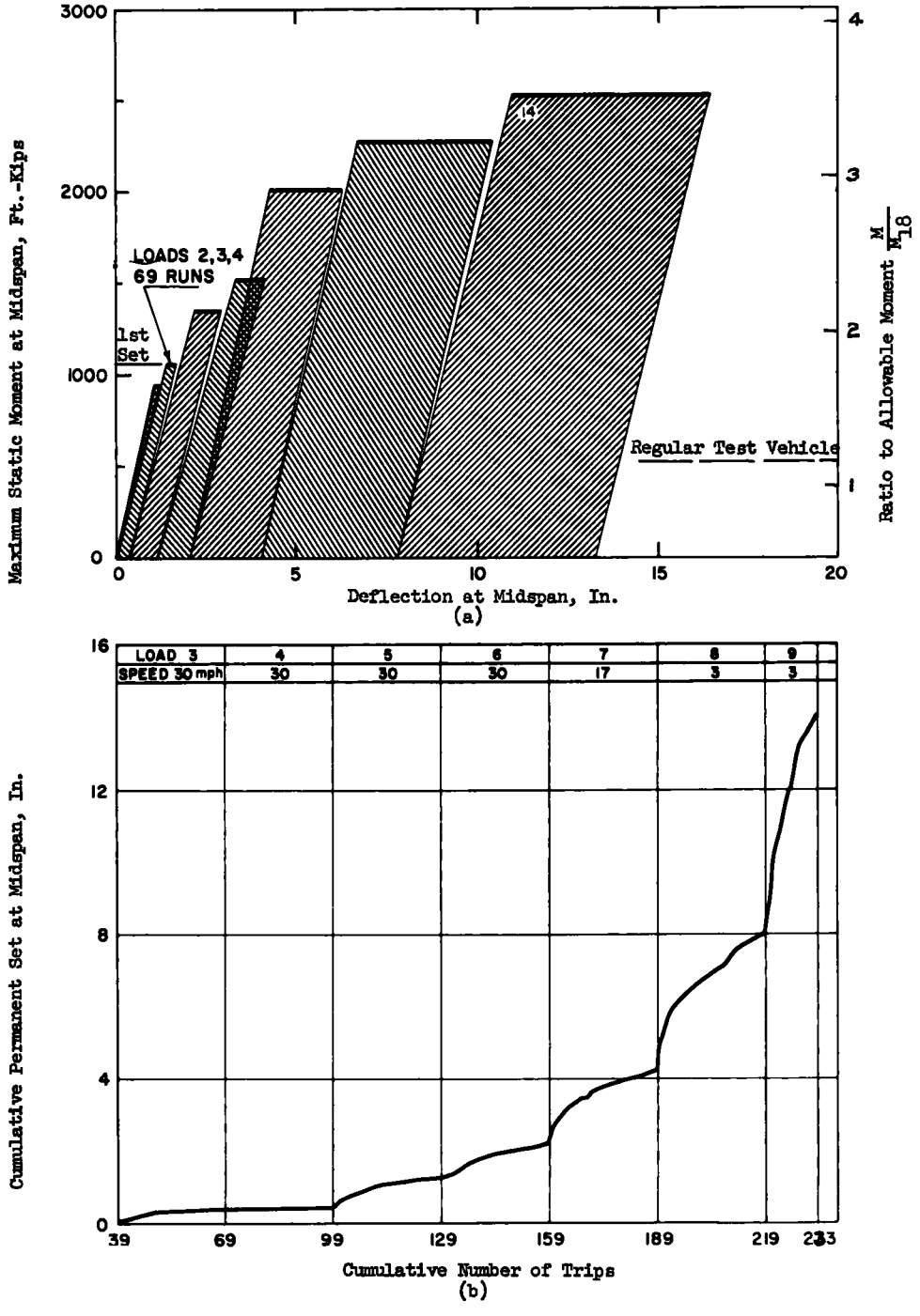

Figure 9. Moment-deflection and set-trip diagram, composite steel bridge 3B.

was also noted in the fillet of the web where it joins the bottom flange. The yielding was fairly uniform throughout each beam, except that it was slightly more pronounced near the ends of the cover plates.

The rate of permanent deformation was similar to that of the preceding loading in that for the first 10 runs it was about 0.06 in. per run and for the remaining 20 runs was 0.02 in. per run. This decrease of permanent set during the last half of the runs of each loading appears to be typical of each loading.

The large fatigue crack measured 0.14 in. wide after this loading; however, it did not increase in length.

The yield lines during the seventh loading moved up into the web to a height of about 6 in. The vehicle speed was reduced to 17 mph. The

rate of permanent deformation increase was somewhat irregular, ranging from 0.5 in. on the first run to 0.06 in. for some of the later runs.

The large fatigue crack became 2.0 in. long and 0.22 in. wide during the seventh loading. It was therefore butt welded prior to the eighth loading.

During the eighth and ninth loadings the speed of the test vehicle had to be reduced to creep speed due to the heavy axle loads. Because of the slow speed, and therefore the time which would be required for turning around, the vehicle was driven alternately forward and backward across the bridge with the vehicle facing in the direction of regular test traffic.

Heavy yielding in the web, especially near the ends of the cover plates, resulted during the eighth loading. Tension cracks in the deck, reaching about halfway up from the bottom, were observed at sections located near the ends of the cover plates. The yielding progressed upward from the bottom flange through the web to the top flange, being at all times tensile yielding. The rate of permanent deformation was high on the first few runs (0.80 in. on the first run) and only about 0.03 in. per run on the last three runs. Forward runs produced slightly greater live load deflection and permanent deformations than reverse runs. The total permanent deformation for these 30 runs was about 3.7 inches.

On the first run of the ninth loading yielding was noticed on the top flange near the entrance end of the cover plates, and tension yielding all along the top flange resulted by the fifth run. The tension cracks in the bottom of the deck did not reach the top of the deck. They remained about 2 in. below the top.

The testing was stopped after the fourteenth run of the ninth loading because of the large accumulated permanent deformation, which was 14.1 in. The total permanent deformation caused by the 14 runs of the last loading was 5.5 in.

The deck showed no signs of crushing; neither was there any sign of a separation between the deck and the beams. As was the case with the other steel bridges, more trips could have been made, probably even with a higher load.

Strictly speaking, this bridge did not fail. According to the definition of failure for steel bridges, failure occurred when the permanent deformation at midspan for one run was always greater than that due to the preceding run. Testing was stopped before this could happen. There was the same characteristic reduction in permanent set due to the later runs of the ninth loading as was noted for all other loadings.

At the end of the test, yield lines on the surfaces of the beams indicated tensile yielding through the full depth of the steel section just off both ends of the cover plates. At midspan, tensile yield lines reached the underside of the top flange. The tension cracks in the slab near the ends of the cover plates extended to within 2 in. of the top surface, but there was no sign of the crushing of concrete on the top surface.

The loading that first caused yielding was the first loading, but this yielding was very slight and it was not until the third loading that the permanent set at midspan exceeded 0.1 in. The rear axle loads of the test vehicle during the third loading were, front to back, 32.9, 32.3 and 32.3 kips.

The total moment (live load plus dead load) resulting from the third loading was 1,536 ft-kips at midspan and 1,329 ft-kips at the end of the cover plates. These values were 49 percent and 53 percent in excess of the corresponding moments caused by regular test vehicle No. 61.

The last three axle weights during the ninth loading were, front to back, 72.3, 73.5 and 82.3 kips. The total midspan moment was 2,996 ft-kips and that at the end of the cover plates was 2,739 ft-kips. These values are respectively 190 percent and 215 percent in excess of the corresponding moments caused by regular test vehicle No. 61.

Figure 10 shows the bridge at the end of the test to failure with increasing loads. This was the only composite steel bridge tested to failure with increasing loads.

Reinforced Concrete Bridge 8A

The reinforced concrete bridge 8A was located in the same loop and in the same lane as composite steel bridge 3B, and was therefore also subjected to passages from vehicle 61 during the regular test period.

A cross-section at midspan and some details of bridge 8A are shown in Figure 11. The main tensile reinforcement consisted of Nos. 8, 9 and 11 deformed bars made of intermediate grade steel conforming to ASTM Designation A15-54T and had diamond-shaped deformations. The yield points of the above bars as determined from tensile tests in the laboratory were, respectively, 52.6, 51.8 and 49.5 ksi. The webs were reinforced with vertical stirrups made of No. 3 bars and spaced as shown. They were omitted from the center portion of the beams.

Just prior to the test to failure all three beams were cracked in tension. Some of the cracks near midspan reached up to the bottom of the deck; details of crack spacing and width can be found in AASHO Road Test Report No. 4 (HRB Special Report 61D).

During the time of regular testing, bridge 8A was subjected to 558,400 passages of regular test vehicle No. 61. In addition to this, about 1 million more stress applications were put on during the accelerated fatigue test.

Figure 10. Yielding of composite beams, midspan.

TABLE 5

COMPUTED MAXIMUM STATIC MOMENTS AND MEASURED AXLE LOADS, BRIDGE 8A

Load	No. of Runs	Midspan Moment (ft-kips)	Axle Loads (kips)						
			1	2	3	4	5	6	7
Dead		653							
Veh 61[1]		450	8.9	30.2	29.9				
1	30	750	14.1	14.1	16.6	17.8	21.7	22.1	24.0
2	30	1,030	14.5	13.6	18.6	18.7	29.2	30.1	33.1
3	30	1,190	14.1	14.0	18.2	18.9	32.3	35.3	39.2
4	30	1,390	13.6	13.7	24.2	24.7	37.5	41.2	47.8
5	2	1,550	14.5	14.0	30.9	30.3	43.0	44.9	52.8

[1] Regular test vehicle 61.

Five separate loadings were used during the test to failure. The axle loads and the computed dead load and static midspan moments are given in Table 5, which also includes the axle loads and computed moment produced by regular test vehicle No. 61.

The moment-deflection and set-trip diagrams are shown in Figure 12. The average recorded stresses and deflections are given in Table 6 for each loading except the last one, because by that time all strain gages had been destroyed. The live load stresses shown are derived from measured strains in the bottom layer of reinforcement. The values in parentheses, when added to the computed dead load stress (also given in Table 6) exceed the yield

TABLE 6

STRESSES AND DEFLECTIONS, BRIDGE 8A

Load	Elastic Live Load Deflection (in.)	Midspan Stresses[1] (ksi)		
		Interior Beam	Center Beam	Exterior Beam
Dead		16.4	17.0	20.0
Veh 61[2]	1.07	15.9	15.2	14.9
1	1.40	22.9	22.2	21.0
2	1.85	31.7	31.3	(30.2)
3	2.15	(37.4)	(37.8)	(37.0)
4	2.55	(97.9)	(54.0)	(70.0)
5	3.00	Gages destroyed		

[1] Values in parentheses when added to the dead load stress exceed the yield point; yield point of No. 11 bars, 49.5 ksi.

[2] Regular test vehicle 61.

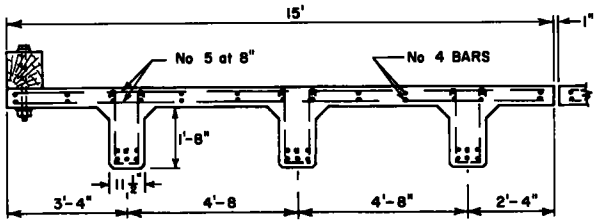

Section at Midspan

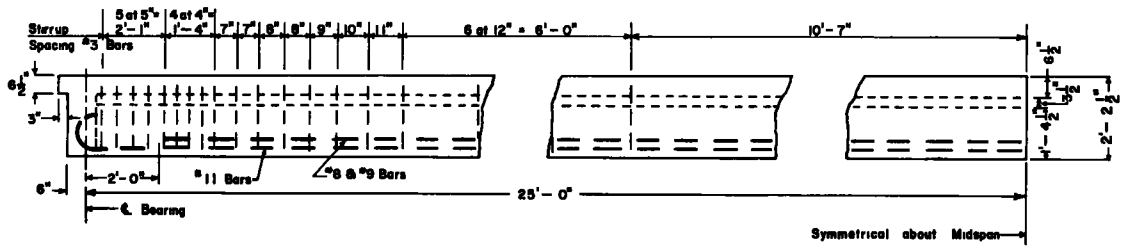

BEAM REINFORCEMENT

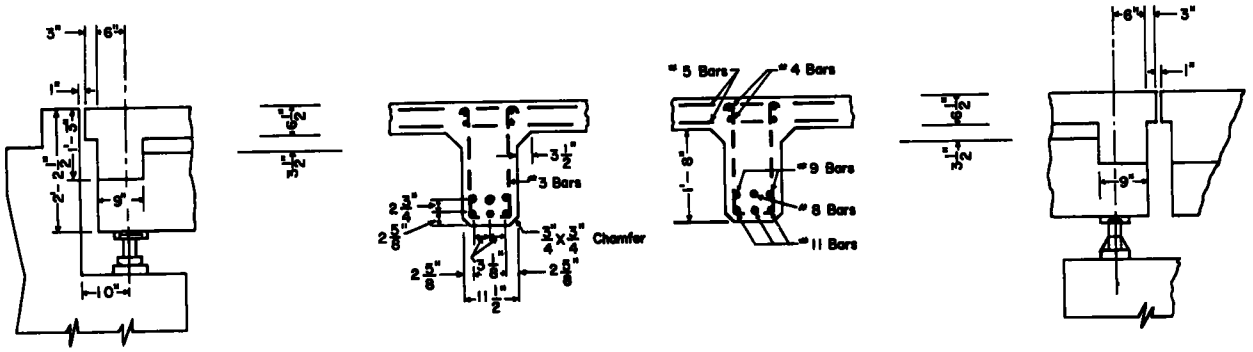

Figure 11. Details of reinforced concrete bridge 8A.

point of the bars in the bottom layer of reinforcement and are therefore not true stresses.

The first two loadings produced no permanent deformation and no difference in the appearance and behavior of the bridge was noted. Figure 12 shows that the beams retained their elastic behavior during these loadings. There was only a trace of permanent set during the third loading, but the fourth loading produced heavy yielding and diagonal shear cracks appeared near the third points on all three beams.

The only visible indication of the yielding of the reinforcing steel was the appearance of permanent set and the widening of the cracks in the concrete beams.

The cracks near midspan widened noticeably during the fourth loading and on the eighteenth run were seen to reach very near to the top of the deck. The set-trip diagram (Fig. 12b) shows that the rate of permanent deformation increased with each run, going from 0.02 in. on the first run to over 1.0 in. on the last four runs. The total permanent deformation during the fourth loading was about 10.8 in.

On the first run of the fifth loading, the midspan crack was visible on top of the deck and on the next run the deck failed in compression. Most likely failure would have occurred with the fourth loading, if a few more runs had been made. It is evident in Figure 12b that the rate

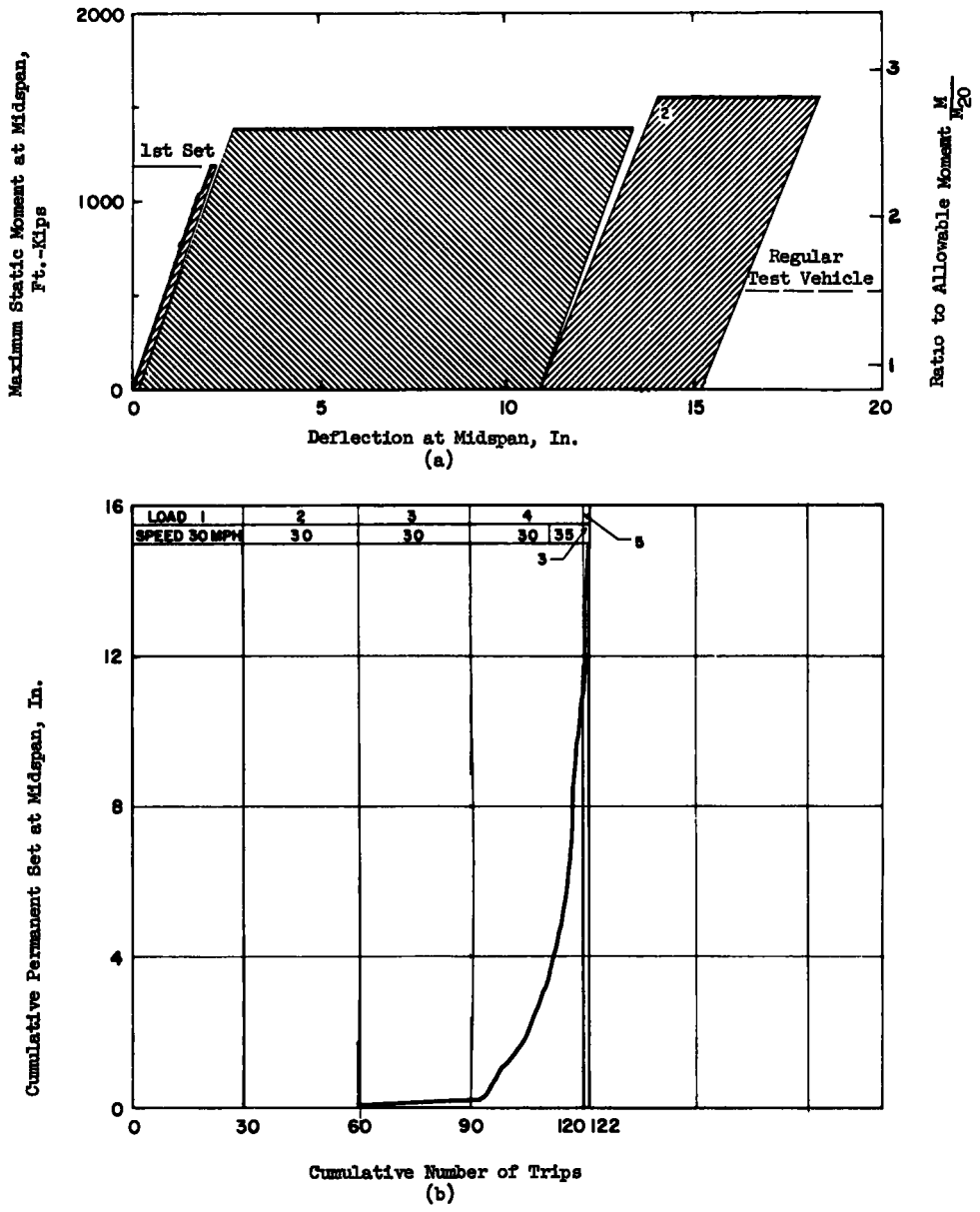

Figure 12. Moment-deflection and set-trip diagram, reinforced concrete bridge 8A.

of permanent deformation during the fourth loading continued to increase with each run. The permanent deformation at midspan just before failure was 15.0 in. Figure 13 shows the bridge at failure.

The loading that produced the first signs of yielding was the third loading. The weights of the last three axles of the test vehicle during this loading were, front to back, 32.3, 35.3 and 39.2 kips. The total midspan moment (live load plus dead load) in the third loading was 1,843 ft-kips. This value exceeded the moment produced by regular test vehicle No. 61 by 67 percent.

The vehicle rear axle weights at failure were 43.0, 44.9 and 52.8 kips, front to back. The total midspan moment at failure was 2,203 ft-kips. This value exceeded the midspan moment produced by regular test traffic by 100 percent.

There was another reinforced concrete bridge tested to failure with increasingly heavier loads. Bridge 8B was a replicate of bridge 8A and was located in the same traffic lane. The same five loadings used on bridge 8A also crossed 8B, and the behavior during testing of both bridges was very similar.

Yielding on bridge 8B was also noticed first on the third loading and the bridge failed during the fifth loading by crushing of the deck near midspan. However, this did not happen until the 7th run, whereas bridge 8A failed on the second run of the fifth loading.

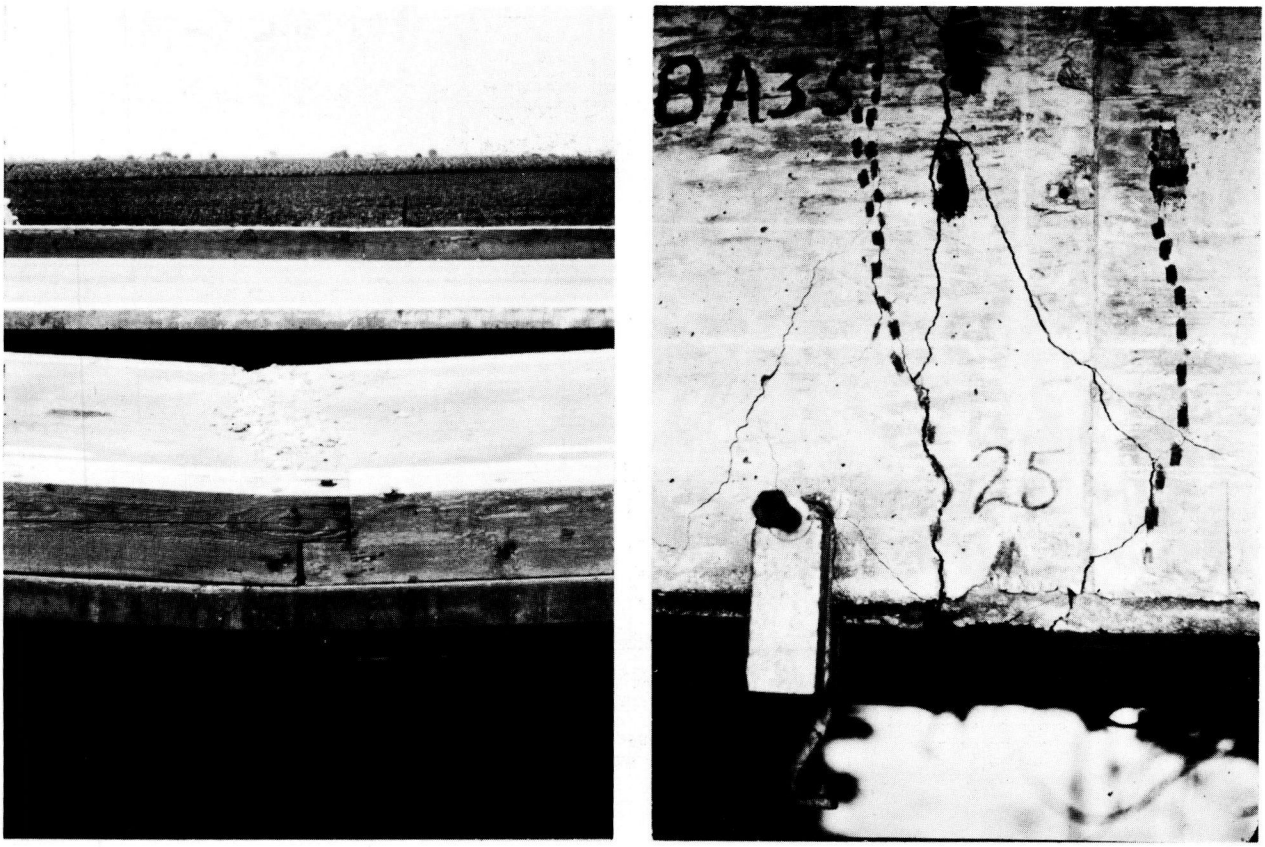

Figure 13. Reinforced concrete bridge after failure, midspan.

The total permanent set at midspan at failure of bridge 8B was over 14 in.

Post-Tensioned Prestressed Concrete Bridge 5A

All four of the prestressed concrete bridges were located at one site. Both post-tensioned bridges were in the tandem-axle vehicle lane during regular testing. Bridge 5A was located on the tangent side and was second in line of traffic.

A cross-section at midspan and some details of bridge 5A are shown in Figure 14.

All of the prestressed concrete beams were precast I-sections. The three beams of bridge 5A were reinforced with draped parallel wire cables. There were four tendons, each containing 10 wires of 0.192-in. nominal diameter in each beam. The tendons were encased in flexible metal conduits, anchored by Freyssinet cone anchorages and grouted. The web reinforcement was made of No. 3 bars extending above the precast beams. The end blocks were reinforced with No. 4 horizontal bars in addition to vertical stirrups.

The yield strength of the steel wires, as determined in the laboratory, was found to be 227.4 ksi and the ultimate strength was 257.3 ksi.

Immediately prior to the test to failure, all three beams were cracked quite uniformly throughout the middle third. The cracks were spaced about 2 ft apart; most of them reached to the top of the beam just under the deck. The width of the cracks, measured when the bridge was unloaded, was around 0.005 in. The slab was in good condition. During the regular test 556,700 passages were made with test vehicle No. 52 (Fig. 1). The nominal axle weights were 9 kips on the front axle and 40 kips each on the tandem axles, producing a gross vehicle weight of 89 kips.

Three increments of loading were used. The loads and the computed static midspan moments are given in Table 7, which includes

TABLE 7

COMPUTED MAXIMUM STATIC MOMENTS AND MEASURED AXLE LOADS, BRIDGE 5A

Load	No. of Runs	Midspan Moment (ft-kips)	Rear Axle Loads (kips)			
			4	5	6	7
Dead		654				
Veh 52[1]		520	20.0	20.0		
1	30	570		16.7	17.2	17.9
2	30	1,000		28.8	30.0	32.0
3	35	1,315		37.1	38.9	41.6

[1] Regular test vehicle 52.

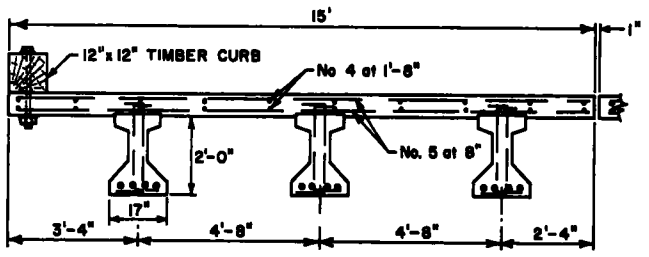

Section of Bridge 5A at Midspan

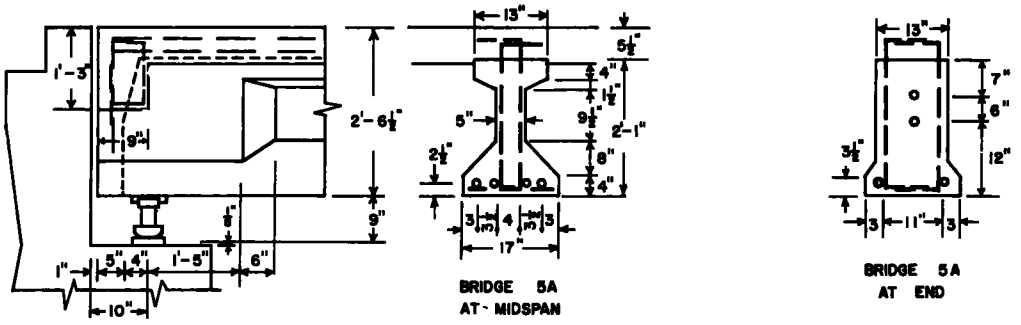

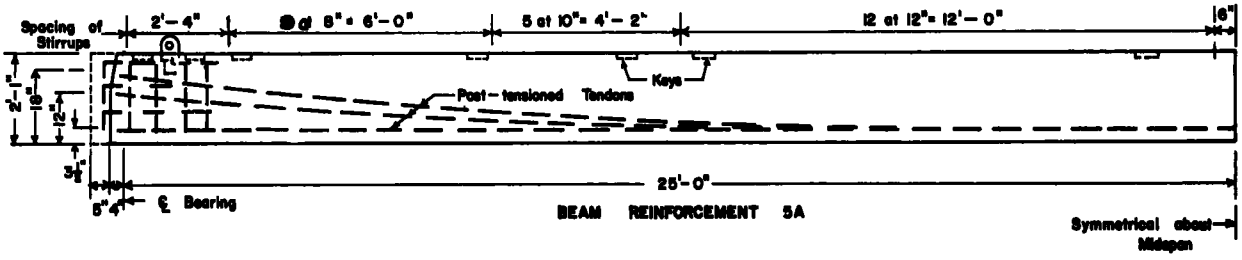

Figure 14. Details of bridge 5A.

loads and moments produced by a regular test vehicle, as well as the computed dead load moment.

Because there were only three loadings and also because some of the gages were destroyed before the end of the test, few live load stresses were recorded. However, Table 8 gives the available information on live load stresses. The effects produced by regular test vehicle No. 52 are included for comparison, as are the computed dead load stresses. All of the stresses refer to the bottom layer of prestressing steel at midspan. The dead load stresses are for an uncracked section just before beginning of regular test traffic. The recorded live load stresses and deflections produced by vehicle 52 are characteristic of the end of the regular testing period. The stresses differ slightly from those recorded near the beginning of regular testing and the deflections are about twice as large (0.85 in. near the end; 0.44 in. at the beginning) due to the cracking of the beams.

Under the first loading, no permanent deformation was observed, nor were there any new cracks noted, but the existing ones opened up somewhat. The moment-deflection relationship

TABLE 8

STRESSES AND DEFLECTIONS, BRIDGE 5A

Load	Elastic Live Load Deflection (in.)	Midspan Stresses[1] (ksi)		
		Exterior Beam	Center Beam	Interior Beam
Dead [2]		146 7	144 8	144 9
Veh 52[3]	0 85	22 2	19 8	25 4
1	0 57	23 6	17 7	21 0
2[2]	2 01	(93 8)	66 3	75 3
3	6 00	(90 3)	(143 9)	—

[1] The values in parentheses when added to the dead load stress exceed the yield strength; yield strength of prestressing wires, 227 4 ksi.
[2] For an uncracked section just prior to beginning of regular testing.
[3] Regular test vehicle 52.

and the set-trip diagram are shown in Figure 15. A small amount, 0.09 in. for 30 runs, of permanent set resulted from the second loading, and the existing cracks again became wider. The recorded stresses show yielding only in the exterior beam. When the recorded stress for the exterior beam (Table 8, loading No. 2) is added to the dead load stress, the sum exceeds the yield strength of the prestressing wires.

The first run of the third loading produced a permanent set at midspan of about 0.1 in. The set continued to increase with each succeeding trip of the test vehicle, going as high as 1.4 in. on the next to last run.

At intervals, during the third loading the width of the cracks near midspan was measured on the unloaded bridge. On the sixth trip they were about 0.06 in. wide on the bottom flange, on the 11th trip about 0.09 in. and on the 16th trip about 0.18 in. A few of the cracks near midspan had reached the top of the slab by the eighth trip.

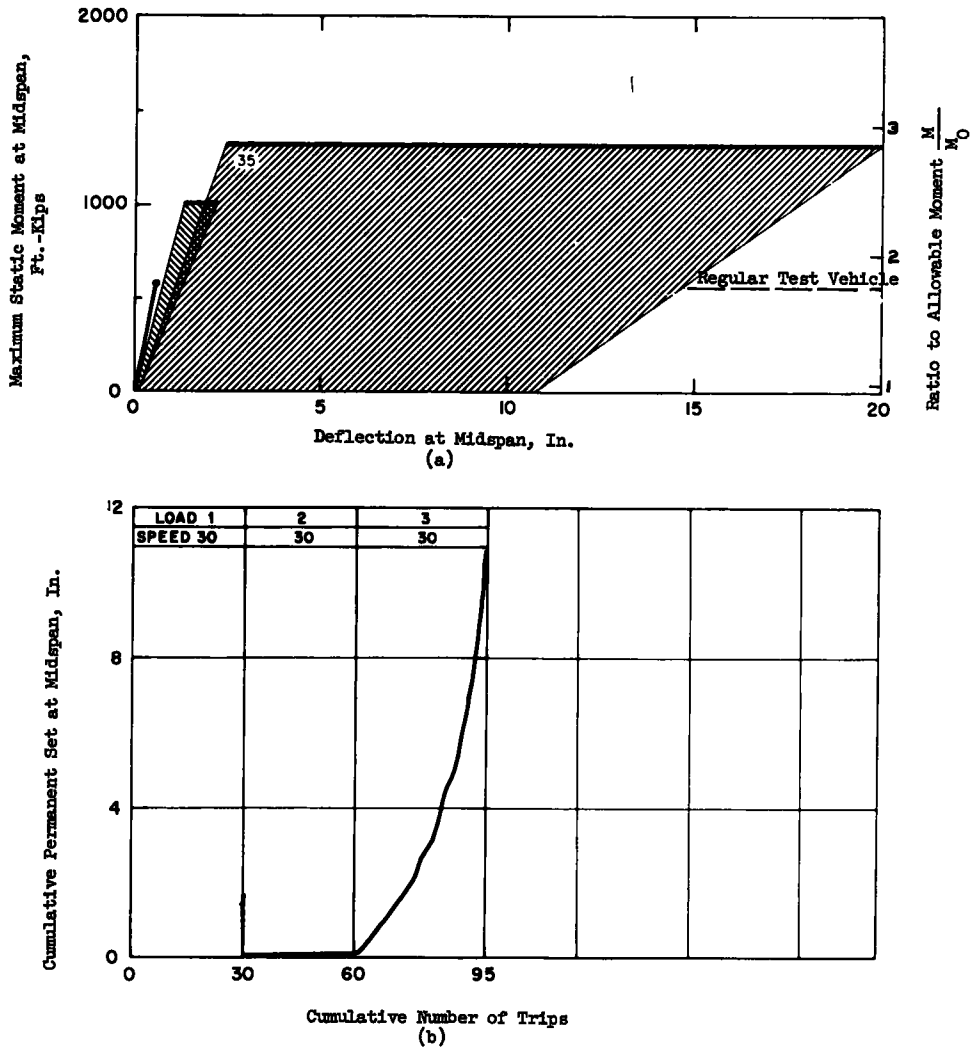

Figure 15. Moment-deflection and set-trip diagram, post-tensioned prestressed concrete bridge 5A.

The bridge failed during the thirty-fifth run by crushing of the deck at a point about 7 ft west of midspan. The failure was caused by excessive deformation resulting from loss of bond and from yielding of the wire cables.

The extent of the loss of bond was investigated by breaking away the concrete around the conduit for about 6 ft near midspan of the exterior beam. The conduit was peeled away from the grouted wires and it was then seen that there was no bond left because the grout crumbled and fell away from the wires as soon as it was exposed. A shorter section of conduit, about 2 ft long, from the uncracked portion of the beam near the abutment was also investigated. No loss of bond was discovered when the conduit was peeled away; in fact, it was difficult to break the grout away from the wires by hand.

In both of the sections of cable, no voids were discovered in the grouting and there were no bare spots on the wires that had not been covered with grout. Figure 16 shows bridge 5A after failure.

Yielding was first noticed during the second loading. The rear axle weights of the test vehicle during this loading were 28.8, 30.0 and 32.0 kips. The total midspan moment of 1,654 ft-kips was 41 percent greater than the corresponding moment produced by the regular test vehicles.

The total midspan moment at failure was 1,969 ft-kips; this was 68 percent in excess of the moment produced by the regular test vehicles.

It should be pointed out that the mode of failure of bridge 5A was unique among the prestressed concrete bridges. The three other prestressed bridges failed by the breaking of the steel reinforcement near midspan, and in no case was any loss of bond noted.

Bridge 5B, the other post-tensioned prestressed concrete bridge was located in the same traffic lane as bridge 5A. However, it was designed for only 300-psi tension in the bottom fiber of concrete as contrasted with 800 psi in bridge 5A.

Bridge 5B was also tested to failure with increasingly heavier loads. There were no cracks visible by an unaided eye in the beams resulting from regular test traffic or the accelerated fatigue test.

Eight loadings were used in the test to failure. Permanent set was observed during the sixth loading. The total midspan moment produced during this loading was 2,662 ft-kips, which was 118 percent above the moment produced by the regular test vehicles.

The bridge failed by rupture of the prestressing steel near midspan during the eighth loading. However, 71 trips were made with this loading before the bridge collapsed. The total moment at failure was 3,172 ft-kips; this was 160 percent above the corresponding midspan moment produced by the regular test traffic.

No indication of bond failure was observed at any time during the test to failure. There was some separation of the deck from the beams, first noticed during the seventh loading, and extending over about the middle third of the bridge at the time of failure.

The difference in behavior between the two post-tensioned bridges would indicate that a primary factor contributing to the bond failure in bridge 5A, was the fact that the beams of this bridge were cracked throughout the regular testing period. Extensive cracking was not noted on bridge 5B until the second loading of the test to failure with increasing loads.

Pretensioned Prestressed Concrete Bridge 6B

Bridge 6B was located in the single-axle vehicle lane and was subjected to traffic from regular test vehicle No. 51 (Fig. 1) during the time of regular test traffic. The nominal axle loads were, front to back, 6, 22.4 and 22 4 kips. A total of 556,800 passages were made across the bridge with the regular test trucks and two heavier vehicles crossed the structure by mistake, but no apparent damage resulted.

This bridge was also subjected to the accelerated fatigue test and approximately 950,000 cycles of stress were put on with the mechanical vibrator. The total number of stress applications just prior to the test to failure was therefore near 1,500,000.

A cross-section at midspan and some detailed views are shown in Figure 17. The pretensioned beams were reinforced with twenty ⅜-in. 7-wire strands, anchored by bond. The slabs, web reinforcement and end blocks of all prestressed bridges were the same.

The detailed location and placement of the strands, as well as other construction and design details are described in the AASHO Road Test Report 4 (HRB Special Report 61D). The actual dead load stress was about 171.2 ksi in the bottom strands at midspan. The yield strength and ultimate strength of the strands, determined in the laboratory, were 243.0 and 275.2 ksi, respectively.

There were one or two hairline cracks near the bottom of each beam just prior to the test to failure. The cracks were confined to the sides and there was no continuity established between a crack on one side of a beam and a crack on the other side. The bridge was in very good condition.

The test to failure of this bridge was conducted over a period of about 1½ months. The test vehicle for all loadings was the same tank carrier used on most of the other bridges, and except for the last two loadings, the direction of travel was the same as that of the regular test vehicles. The nominal speeds of the test

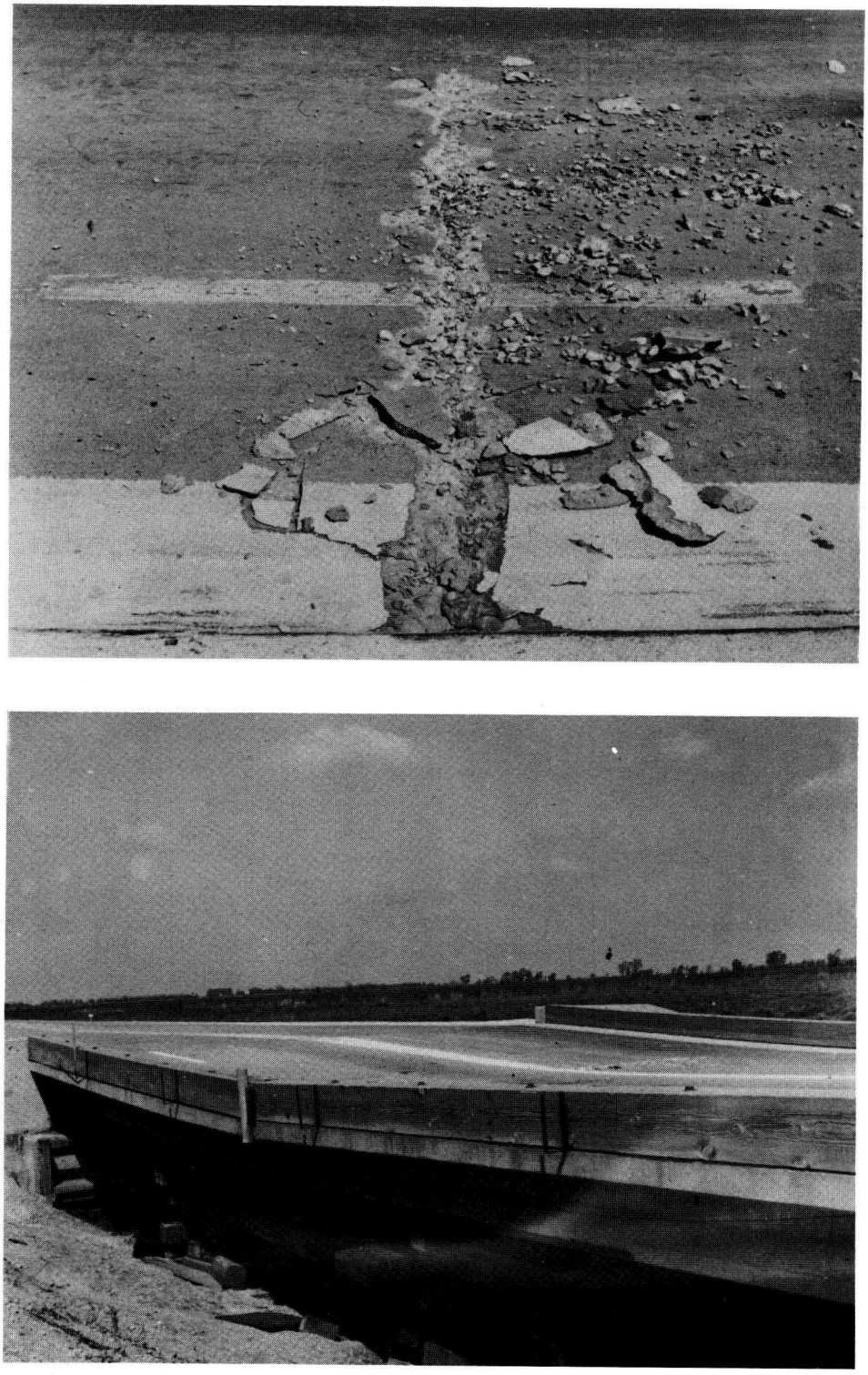

Figure 16. Post-tensioned prestressed concrete bridge 5A after failure.

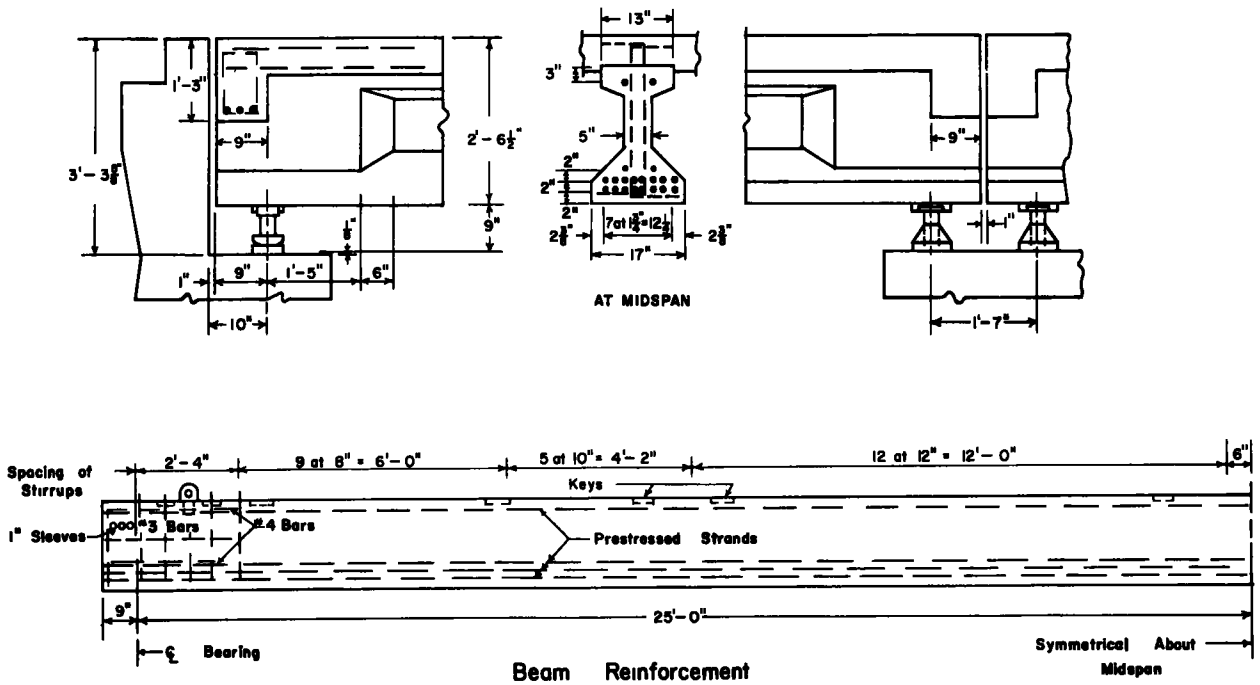

Figure 17. Details of bridge 6B.

TABLE 9

STRESSES AND DEFLECTIONS, BRIDGE 6B

Load	Nominal Speed (mph)	Elastic Live Load Deflection (in.)	Midspan Lower Stress[1] (ksi)		
			Interior Beam	Center Beam	Exterior Beam
Dead[2]			170 1	171 1	172 3
Veh 51[3]	30	0 22	2 4	2 4	2 4
1	30	0 26	4 0	3 5	3 6
2	30	0 37	6 1	5 3	5 8
3	30	0 55	7 3	6 3	5 5
4	30	0 57	7 7	7 5	7 5
5	30	0 88	21 6	19 2	28 2
6	20	1 30	41 9	36 5	43 3
7	16	1 90	60 7	51 5	53 8
8	25	2 50	(77 8)	(75 2)	(73 7)
9	20	3 30	(109 9)	(96 4)	(99 8)
10	20	4 10	(128 0)	(119 9)	(127 4)
11	3	4 85	—	(143 7)	(150 3)
12	3	6 75	—	—	(186 1)

[1] Yield strength of prestressing strands, 243 0 ksi.
[2] In the bottom layer of prestressing steel, before the beginning of regular test traffic.
[3] Regular test vehicle 51.

vehicle during each loading are given in Table 9 along with the recorded live load stresses and deflections. For comparison, stresses produced by regular test vehicle 51, and the computed dead load stress are also included. All stresses refer to the bottom prestressing strands at midspan. The dead load stress is for an uncracked section before the beginning of regular testing.

Twelve separate loadings were used on this bridge. The axle loads, the dead load moment and the maximum midspan static moments computed from the axle loads are given in Table 10. Two sets of values are shown for the tenth loading because the vehicle broke down and a slightly different loading resulted after the vehicle was repaired and reloaded. Again, the loads and moment of a regular test vehicle are included to serve as a means of comparison. Figure 18 shows the moment-deflection and the set-trip diagrams.

No visible changes occurred in the bridge

TABLE 10

COMPUTED MAXIMUM STATIC MOMENTS AND MEASURED AXLE LOADS, BRIDGE 6B

Load	Midspan Moment (ft-kips)	Axle Loads (kips)						
		1	2	3	4	5	6	7
Dead	653							
Veh 51[1]	350	5 6	22 8	22 6				
1	560	—	—	17 0	18 3	16 0	16 9	17 5
2	820	14 0	14 0	17 2	18 5	23 5	24 8	25 4
3	1,000	14 5	13 4	18 4	19 7	28 3	30 0	32 5
4	1,130	13 8	14 0	20 8	20 2	32 0	34 1	37 0
5	1,300	13 5	14 0	27 6	26 0	37 1	38 9	41 6
6	1,400	13 8	14 2	25 5	27 8	39 2	41 0	47 2
7	1,500	14 2	14 0	24 4	23 5	41 7	45 0	49 1
8	1,570	14 2	14 4	29 3	30 7	44 8	46 5	51 2
9	1,780	14 0	14 4	29 2	29 8	48 2	52 0	60 7
10[2]	1,950	14 2	13 9	27 4	36 9	55 0	56 9	65 2
	2,010	—	—	—	—	55 7	57 3	68 0
11	2,270	14 2	14 2	31 0	31 0	62 9	66 6	75 0
12	2,520	13 8	13 9	31 5	30 6	72 3	73 5	82 3

[1] Regular test vehicle 51.
[2] Vehicle broke down during test and was reloaded to values shown in lower line.

during the first four loadings but several small cracks appeared near midspan during the fifth loading.

The moment-deflection diagram (Fig. 18a) indicates that there was a change of slope during the fifth loading. It is also evident from the recorded stresses that there was a change in the stiffness of the beams; *i.e.*, the stresses changed suddenly from around 7.5 ksi to over 25 ksi. Both these changes coincide with the appearance of visible cracks near midspan.

The bridge retained its elastic behavior from the fifth through the eighth loading, but the beams became more and more cracked. A crack study was made during the eighth loading and new cracks and crack advances were marked. After the 30 runs of this loading, approximately the middle 20 ft of each beam had cracks, spaced 12 to 18 in. apart, and those near midspan reached to just under the deck. As yet there was no sign of any permanent set.

A similar crack study during the ninth loading revealed about 10 new cracks per beam, most of them being outside the previously cracked region, which after 30 runs extended about 13 ft on each side of midspan. The cracks near midspan reached about halfway up into the deck.

A small amount of permanent deformation resulted during the ninth loading, about 0.1 in. for the 30 runs.

During the tenth loading, because of the heavy load the vehicle speed was reduced to creep speed, and the truck was driven back and forth across the bridge to avoid turning movements.

Several new cracks outside the previously cracked region were noted during the tenth loading, but the midspan cracks did not extend any higher into the deck. There was a total of 0.3 in. of permanent set during this loading.

A peculiar behavior of the bridge during the heavier loadings is of interest. As soon as the test vehicle had crossed, the bridge rebounded quickly and violently, hitting the abutment with great force, causing some spalling of concrete. The quick rebound was due to the rapid closure of the cracks by the prestressing force, and necessitated a reduction of speed of the test vehicle.

During the eleventh loading, several diagonal shear cracks appeared near the third points of the beams. On about the twentieth run the slab was beginning to separate from the beams near the top of the diagonal shear cracks. The separation was progressing towards midspan. The tension cracks near midspan still extended only half way up into the slab, but were becoming wider. The rate of permanent deformation was about 0.04 in. per run for the forward runs and 0.02 in. for the reverse runs. A total set of 0.7 in. was recorded for 30 runs.

With the twelfth and final loading, 44 runs were made before the midspan cracks were visible on top of the deck.

On the forty-sixth run, the bridge collapsed with a loud noise and fell onto the cribbing. As far as could be determined, all strands had broken in all beams near midspan. During the last run the slab had pulled away from the beams for about the middle third of the bridge.

The rate of permanent deformation was fairly uniform for the first 30 runs (0.08 in. to 0.10 in. per run) and increased during the last 15 runs. Again, the forward runs produced larger deformations than the reverse runs. The total permanent deformation for all runs, just before

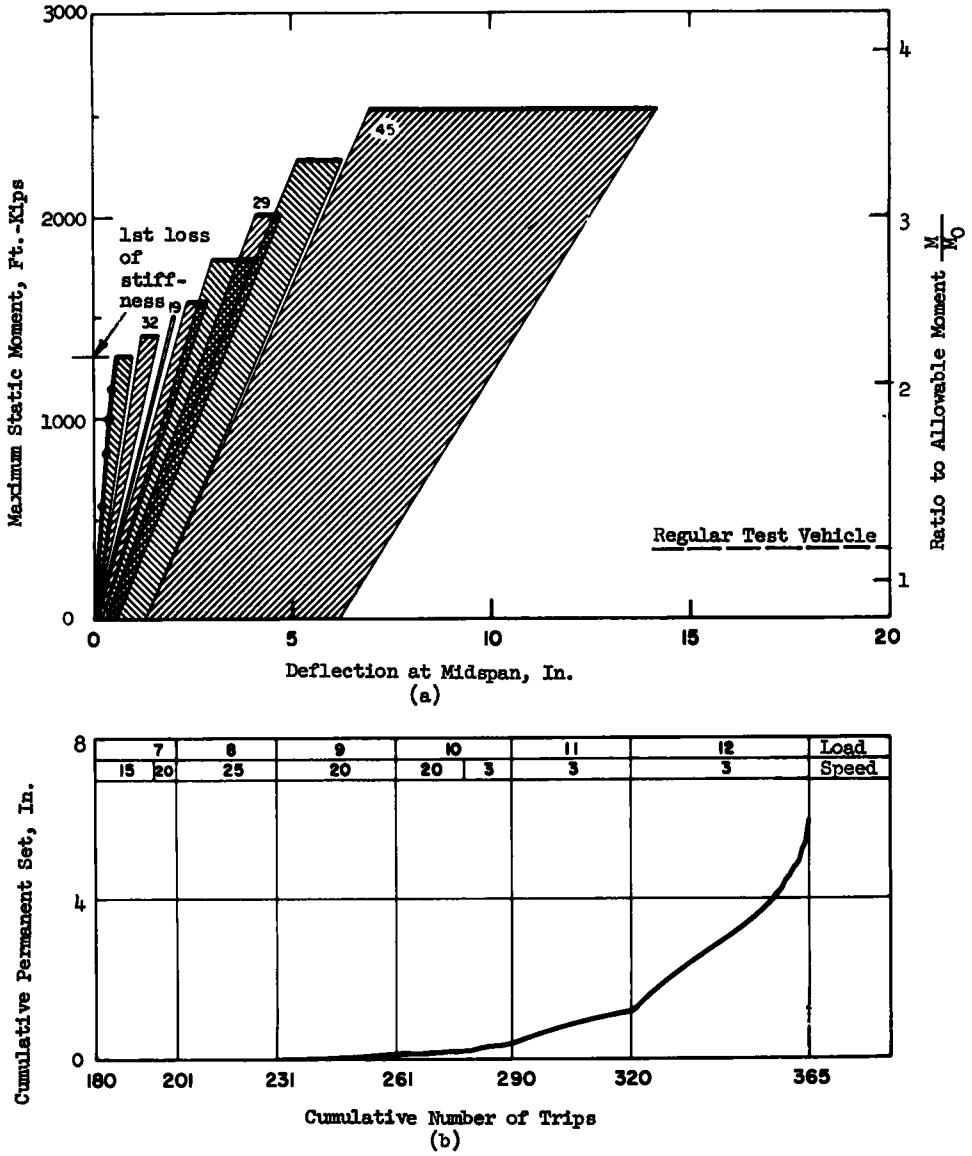

Figure 18. Moment-deflection and set-trip diagram, pretensioned prestressed concrete bridge 6B.

the bridge collapsed, was 6.4 in. Figure 19 shows the failed structures.

The test to failure of this bridge afforded an excellent opportunity for studying and observing the behavior of a prestressed concrete beam in all three phases of its life. That is, through the first four loadings the beams were uncracked, having a certain stiffness, and from the fifth through the eighth loading they were cracked, being less stiff but still retaining their elastic behavior. From the ninth loading on yielding took place and the beams then were in the last, plastic phase of behavior. Figure 20 plots the midspan moment as a function of the recorded live load stress in the lower strands at midspan.

As mentioned, the fifth load produced a cracked section. The total midspan moment produced during this loading was 1,953 ft-kips, and this was 95 percent above the moment produced by regular test vehicles. The moment during the ninth loading, which produced yielding, was 2,433 ft-kips; this was 143 percent greater than the total moment produced by regular test vehicles. The moment during the twelfth loading was 3,173 ft-kips; this moment exceeded the corresponding moment produced by regular test vehicles by 217 percent.

As was the case with several of the other bridges, most likely one higher loading could have been used on the bridge because it took more than 30 runs with the twelfth loading to

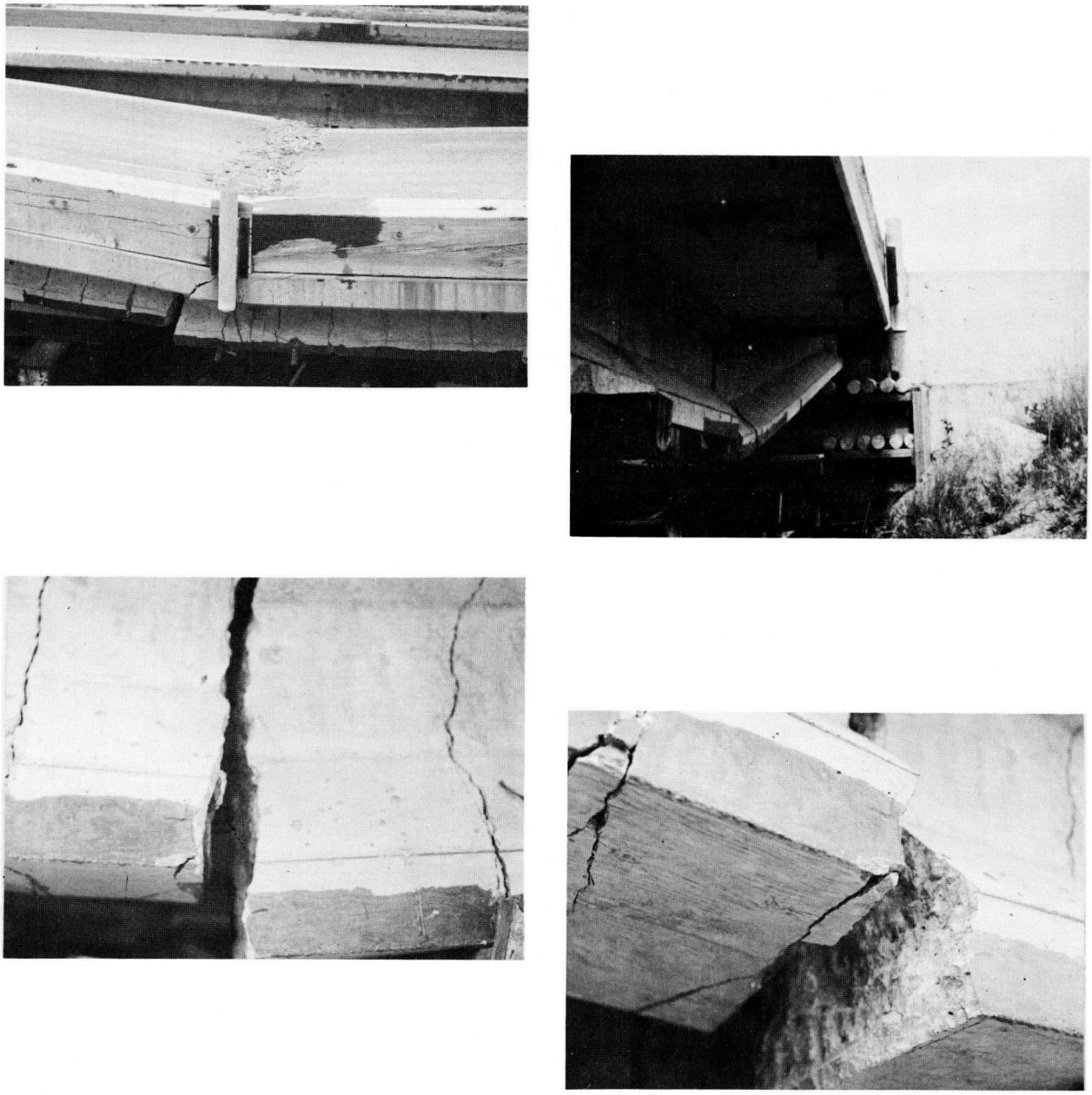

Figure 19. Pretensioned prestressed concrete bridge 6B after failure.

fail it. However, the limitations of the test vehicle did not allow any higher loads.

The other pretensioned prestressed concrete bridge, 6A, was also tested to failure with increasingly heavier loads. The beams of this bridge were cracked to some extent during the regular test. The cracks were spaced about 10 in. apart and were generally confined to the vertical surfaces of the bottom flange. The accelerated fatigue test produced no changes in the cracks.

Bridge 6A was designed for 800-psi tension in the bottom fiber of concrete.

Seven increments of load were used in the test to failure. The third loading produced the first permanent set at a total midspan moment of 1,646 ft-kips, which was 65 percent greater than the moment produced by regular test vehicle 51. The bridge failed by rupture of the prestressing strands near midspan on the nineteenth run of the seventh loading. The total midspan moment at failure was 116 percent above that produced by the regular test traffic and amounted to 2,146 ft-kips. There was no evidence of bond failure at any time.

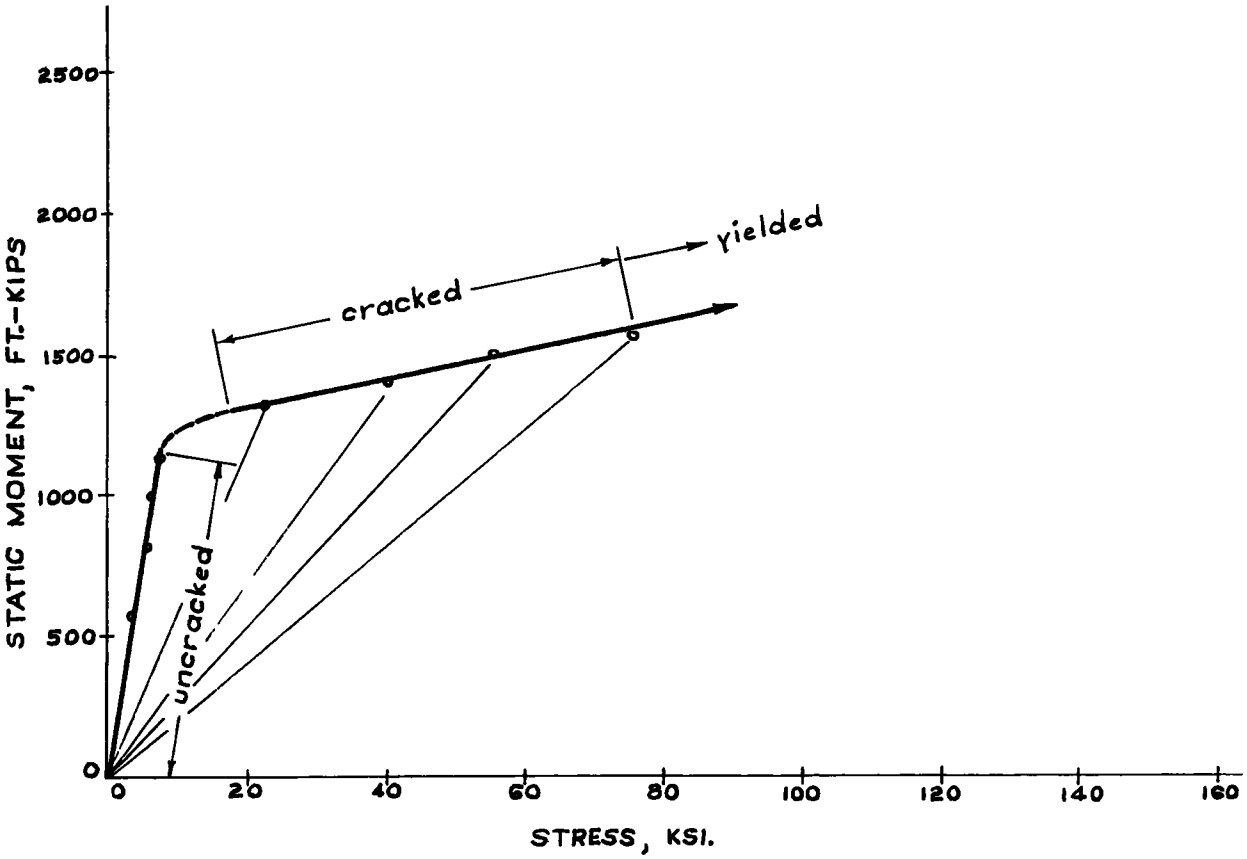

Figure 20. Moment-stress diagram, bridge 6B.

COMPARISON OF CALCULATED ULTIMATE STRENGTH WITH STATIC MOMENTS AT FAILURE

It should be pointed out that a direct comparison of the maximum loads of the various types of bridges tested is meaningless. One cannot ask the question: "Were the prestressed concrete bridges stronger than the steel beam bridges?" or similar questions, because each type of bridge was designed for different loadings or stresses. Only the replicate bridges, 8A, 8B and 9A, 9B, can be compared directly and except for very minor differences, it can be said of them that they behaved essentially the same during testing and failure.

However, the ultimate strength of each bridge can be compared with the computed ultimate capacity as determined by the usual methods of ultimate strength theory.

Reinforced Concrete Bridges

The ultimate strength of reinforced concrete bridges was computed on the assumption that all reinforcing bars below the neutral axis yielded before failure.

$$M_u = \left(1 - 0.59\frac{\Sigma F}{b_s \bar{d} f_c'}\right)\Sigma(Fd) \qquad (1)$$

in which

M_u = ultimate moment resistance;

$$\Sigma F = 3A_1 f_y' + 3A_2 f_y'' + A_3 f_y''' \qquad (2)$$

$$\Sigma(Fd) = 3A_1 f_y' d_1 + 3A_2 f_y'' d_2 + A_3 f_y''' d_3 \qquad (3)$$

$$\bar{d} = \frac{\Sigma(Fd)}{\Sigma F} \qquad (4)$$

b_s = over-all slab width;

f_c' = compressive strength of concrete;

A_1 = area of reinforcement in bottom layer in one beam;

A_2 = area of reinforcement in second layer in one beam;

A_3 = area of longitudinal bottom reinforcement in slab;

d_1, d_2, d_3 = distance from a layer of tension reinforcement to top surface of slab; and

f', f'', f''' = yield point of a layer of tension reinforcement.

Prestressed Concrete Bridges

Two different procedures were used for computing the ultimate strength of prestressed concrete bridges: one assuming fully bonded con-

dition, the other assuming no bond between the prestressing steel and the surrounding concrete.

For bonded beams, it was assumed that failure occurred when the bottom layer of prestressing steel ruptured.

$$M_u = \left(1 - 0.6\frac{\Sigma F}{b_s \bar{d} f_c'}\right)\Sigma(Fd) \qquad (5)$$

in which

$$\Sigma F = 3A_1 f_s' + 3A_2 f_{s2} + 3A_3 f_{s3} + 3A_4 fy' + A_5 fy'' \qquad (6)$$

$$\Sigma(Fd) = 3A_1 f_s' d_1 + 3A_2 f_{s2} d_2 + 3A_3 f_{s3} d_3 + 3A_4 f_y' d_4 + A_5 f_y'' d_5 \qquad (7)$$

A_1, A_2, A_3 = area of the bottom, second and third layer of prestressing steel in one beam;

A_4 = area of mild steel bar (stirrup hanger) in the bottom flange of one beam;

A_5 = area of longitudinal bottom reinforcement in the slab;

$d_1 \ldots d_5$ = distance from a layer of tension reinforcement to the top surface of the slab;

f_s' = ultimate strength of prestressing reinforcement;

f_{s2} = stress in second layer of prestressing steel corresponding to strain $\varepsilon_{su}\dfrac{d_2 - a_s}{d_1 - a_s}$

f_{s3} = stress in third layer of prestressing steel corresponding to strain $\varepsilon_{su}\dfrac{d_3 - a_s}{d_1 - a_s}$

ε_{su} = strain at failure of prestressing steel;

$$a_s = \frac{\Sigma F}{0.7\, b_s f_c'} \qquad (8)$$

f_y', f_y'' = yield point of a layer of tension reinforcement; and M_u, $\bar{d}$, b_s, and f_c' are as previously defined.

For unbonded beams the failure was assumed to occur when the average strain on the top surface of the slab reached the value of 0.0005. Eq. 5 is used, with the terms defined as follows:

$$\Sigma F = 3A_1 f_{s1} + 3A_4 f_y' + A_5 f_y'' \qquad (9)$$

$$\Sigma(Fd) = 3A_1 f_{s1} d_1 + 3A_4 f_y' d_4 + A_5 f_y'' d_5 \qquad (10)$$

f_{s1} = stress in prestressing steel corresponding to strain

$$\varepsilon_p + 0.0005\left(\frac{c_2 f_c' b_s d_1}{\Sigma F} - 1\right);$$

ε_p = strain in prestressing steel caused by initial prestress;

$$\frac{1}{c_2} = 0.8 + 0.0001 f_c' \qquad (11)$$

and the other notations have the same meaning as for beams with bonded reinforcement.

Steel Bridges

The ultimate strength of steel bridges was computed assuming fully plastic stress distribution in the steel and using the static yield point for the wide-flange sections and the cover plates.

Full interaction between the slab and the beams was assumed for the composite bridges:

$$M_u = 3\,[A_p{}^b f_y{}^b (0.5\, t_p{}^b + 2\, t_f + d_w + t_s - 0.5\, a_s) + (2A_f f_y{}' + A_w f_y{}^w)(0.5\, d_w + t_f + t_s - 0.5\, a_s)] + A_r f_y{}^r (d_r - 0.5\, a_s) \qquad (12)$$

in which

M_u = ultimate moment resistance;

$A_p{}^b, A_f, A_w$ = areas of bottom cover plate, one flange, and web of one beam;

A_r = area of bottom longitudinal reinforcement in slab;

$f_y{}^b, f_y{}', f_y{}^w, f_y{}^r$ = static yield point of bottom cover plate, flanges, web, and reinforcing bars;

$t_p{}^b, t_f, t_s$ = thickness of bottom cover plate, flange, and slab;

d_w = depth of web;

$$a_s = \frac{3\,(A_w f_y{}^w + 2A_f f_y{}' + A_p{}^b f_y{}^{pb}) + A_r f_y{}^r}{0.85\, f_c' b_s} \qquad (13)$$

d_r = distance from bottom longitudinal slab reinforcement to top of slab;

b_s = total slab width; and

f_c' = compressive strength of concrete.

Independent action of the beams and the slabs was assumed for the noncomposite bridges

$$M_u = 3\,[0.5\, A_p{}^b f_y{}^{pb} (t_p{}^b + 2t_f + d_w + a_w) + 0.5\, A_p{}^t f_y{}^{pt} (t_p{}^t + 2t_f + d_w - a_w) + 0.5\, A_w f_y{}^w d_w + A_f f_y{}' (t_f + d_w)] + A_r f_y{}^r d_r\left(1 - 0.59\frac{A_r f_y{}^r}{b_s d_r f_c'}\right) \qquad (14)$$

in which

$A_p{}^t$ = area of top cover plate, one beam;

$f_y{}^{pt}$ = static yield point of top cover plate;

$t_p{}^t$ = thickness of top cover plate;

$$a_w = \frac{A_w f_y{}^w + A_p{}^t f_y{}^{pt} - A_p{}^b f_y{}^{pb}}{2t_w f_y{}^w} \qquad (15)$$

t_w = web thickness; and

other notations have the same meaning as for composite beams.

TABLE 11

ULTIMATE STRENGTH OF TEST BRIDGES

Bridge	Dead Load Moment, M_{DL}		Maximum Truck Moment, M_{LL}[1]		Computed Ultimate Strength, M_u		Ratio $\frac{M_{LL}+M_{DL}}{M_u}$	
	Midspan (ft-kips)	End Plate (ft-kips)	Midspan (ft-kips)	End Plate (ft-kips)	Midspan (ft-kips)	End Plate (ft-kips)	Midspan	End Plate
				(a) STEEL				
1A	471	392	1,000	900	1,158	978	(1 27)	1 32
3B	476	409	2,520	2,330	2,733	2,194	(1 10)	1 25
9A	521	461	1,535	1,490	2,008	1,580	(1 02)	1 23
9B	511	452	1,580	1,520	2,007	1,579	(1 04)	1 25
				(b) PRESTRESSED CONCRETE				
5A	654	—	1,315	—	2,215[2]	—	0 89	—
					2,041[3]	—	0 96	—
5B	652	—	2,520	—	3,043	—	1 04	—
6A	646	—	1,500	—	2,109	—	1 02	—
6B	653	—	2,520	—	2,731	—	1 16	—
				(c) REINFORCED CONCRETE				
8A	653	—	1,550	—	2,122	—	1 04	—
8B	653	—	1,550	—	2,110	—	1 04	—

[1] Static moment caused by the test vehicle.
[2] Assuming full bond between the prestressing steel and the concrete.
[3] Assuming no bond between the prestressing steel and the concrete.

Comparison of Calculations with Tests

The computed ultimate strengths are compared with the test data in Table 11, which includes all ten bridges that were tested to failure with increasingly heavier loads.

Table 11 gives moments at midspan and at the end of cover plates for dead load and for the heaviest vehicle that crossed the bridge. The sum of the moments caused by the two external loads is compared with the computed ultimate strength in the last two columns. For every bridge, except 5A, the ratio was larger than unity.

Steel bridges 3B, 9A and 9B were 23 to 25 percent stronger than their computed static fully plastic capacity. This high resistance was developed at the ends of the cover plates; the observed strength at midspan (ratios in parentheses) was only 2 to 10 percent in excess of the computed strength. The corresponding values for bridge 1A were 32 and 27 percent.

The high strengths, large amounts of yielding and the shapes of the diagrams of maximum moments suggest that some strain hardening took place outside the cover plates.

The observed strength of the prestressed concrete bridges 5B and 6A, and of the reinforced concrete bridges 8A and 8B, was 2 to 4 percent in excess of the computed ultimate strength. On the other hand, bridge 5A, which showed signs of bond failure, developed only 89 percent of the strength computed on the assumption of a fully-bonded condition. When absence of band was assumed, the strength ratio for bridge 5A became 0.96.

Bridges 1A and 6B developed substantially higher strength ratios than other comparable test structures, but no factors were found that would explain satisfactorily these large capacities.

The effects of impact were not included in the ultimate strength computations. To a limited extent, the amount of increase in stresses and deflections caused by faster than creep speed runs, was determined. Creep speed effects were used as a base. The reinforced concrete bridges, the noncomposite steel bridges and post-tensioned prestressed concrete bridge 5A all failed while the test vehicle was traveling at faster than creep speed.

The impact percentages varied between bridges from about 15 percent to 28 percent. The magnitude of impact was different when computed from stresses than when computed from deflections.

SUMMARY

In this report the tests to failure with increasing loads were described for one bridge of each type studied at the AASHO Road Test. Ten bridges were tested, three noncomposite steel bridges, one composite steel bridge, two reinforced concrete bridges and four prestressed concrete bridges.

The noncomposite steel bridges yielded first near the approach end of the cover plate, then near the exit end and by the time yielding at midspan took place there was such a large amount of permanent deformation that testing was stopped. Tensile yielding progressed from the bottom flange upward into the web while compressive yielding progressed downward from the top flange into the web. All three of the noncomposite bridges exhibited greater ultimate capacities than the computed ones, the test values ranging from 23 to 32 percent in excess of the computed ones.

The composite steel bridge yielded to within 8 ft of the ends of the beams and yielding was not confined to the ends of the cover plates. Only tensile yielding was observed, progressing from the bottom flange up through the web into the top flange. This was the only bridge that did not fail, according to the definition of failure for steel bridges. Even so, the moment at the end of the cover plates produced by the test vehicle during the last loading was 25 percent greater than the computed ultimate moment.

The reinforced concrete bridges failed by crushing of the deck brought on by yielding of the reinforcing steel near midspan. Both bridges failed quickly once the reinforcing steel began to yield. The ultimate moment due to the test vehicle was only 4 percent greater than the computed ultimate strength.

Bridge 5A, the post-tensioned prestressed concrete bridge, failed by crushing of the deck, probably because of loss of bond between the prestressing wires and the concrete. The midspan moment produced by the test vehicle at failure was slightly below the computed ultimate capacity assuming no bond between the prestressing steel and the concrete.

Post-tensioned bridge 5B and the pretensioned prestressed concrete bridges failed by rupture of the prestressing strands near midspan. No evidence of bond failure was observed. Relatively small amounts of permanent deformation were recorded prior to failure. The midspan moments produced by the test vehicle at failure were from 2 to 16 percent greater than the computed ultimate moments.

CONCLUSION

A direct comparison between the major types of bridges cannot be made; however, certain comparisons between bridges of related design are applicable.

Particularly interesting is a comparison between the composite steel bridge 3B and the noncomposite steel bridges. All four bridges had beams of the same depth, but the weight of the steel sections was 55 lb per ft in bridge 1A, 60 lb per ft in bridge 3B and 96 lb per ft in bridges 9A and 9B. The last two bridges had cover plates on both the top and the bottom flange while the other two had them only on the bottom flange. The strengthening and stiffening effects of the composite action are apparent. The stiffening effect can be seen best on the moment-deflection diagrams; for example, for the moment at midspan of 500 ft-kips the deflections at midspan were: noncomposite bridge 1A, 2.2 in.; composite bridge 3B, 0.6 in.; and noncomposite bridges 9A and 9B, 1.2 in.

The strengthening effect of composite action is illustrated by the values of the maximum static moment at midspan: noncomposite bridge 1A, 1,000 ft-kips; composite bridge 3B, 2,500 ft-kips; noncomposite bridge 9A, 1,535 ft-kips; and noncomposite bridge 9B, 1,580 ft-kips. It is apparent that the differences in beam sizes, impact factors and properties of materials cannot account for the substantially higher stiffness and ultimate moment resistance of the composite bridge 3B.

Another characteristic of composite bridges that was demonstrated by the test of bridge 3B is the shape of the moment-deflection diagram past yielding. Figure 9a shows that the transition from elastic deformations to the maximum load is very gradual so that even relatively large increases of load beyond that causing first yielding will result in only small permanent deformations. This is in a marked contrast with noncomposite bridges (Fig. 7a) in which large permanent deformations occurred at loads not greatly in excess of the yield load. In other words, for a composite bridge the magnitude of the yield load is a less critical quantity than for a noncomposite bridge.

It should be emphasized that all four of the steel bridges, even though badly deformed, could still be used by light vehicles. This could not be said of the other bridges, because they broke into two parts and would have fallen from their supports if it had not been for the cribbing.

One of the two post-tensioned prestressed concrete bridges failed largely because of loss of bond. However, a conclusion that post-tensioned beams are more susceptible to bond failure than pretensioned bridges can not be made because of other differences between the two types of bridges. The loss of bond was probably due more to the combination of cracking and smooth wires than to the method of tensioning. Bridge 5B, the other post-tensioned bridge also had smooth wires but was not cracked until the test to failure and showed no signs of bond failure. Bridge 6A, pretensioned with strand reinforcement, was cracked during the time of regular testing, yet it too showed no signs of bond failure. Bridge 6B, also pretensioned with strands, was not cracked and there were no indications of bond failure.

The behavior during testing and failure of the reinforced concrete bridges agreed very

well with laboratory tests on reinforced concrete beams.

As a whole, it can be said that except for one bridge, all bridges were stronger in varying degrees than the calculated ultimate capacities indicated. However, the main conclusion for all ten bridges tested is that the safe capacities of simple-span, single-lane bridges can be predicted reasonably well from the ultimate strength theories.

This report deals primarily with the "consumptive use" of a bridge. That is, the test bridges were destroyed, or consumed, as they were being used to support increasingly heavier loads. Information was gained on the overload capacity of the bridges at various stages of overloading as well as on the ultimate capacities at failure. This information should not be applied directly to bridges found on the various highway systems of the country, but should serve only as a basis of judgment in estimating the number of overloads of a specified weight above the design loads that should be permitted to cross a particular structure without causing damage, or in cases of national emergencies, to estimate the maximum load that could cross a structure a very limited number of times, if need be at the risk of destroying the usefulness of the structure.

The direct application of overload information, as presented in this paper, to other bridges should be done only after the difference of design and construction between the AASHO Road Test bridges and other structures has been reconciled. Furthermore, the test bridges were constructed, tested and destroyed within four years and any long term weathering effects, and especially any increased deterioration due to weathering that may have been caused by overloads, could not be observed.